UNIVERSITY OF CALIFORNIA
RIVERSIDE

Airborne Exposure to Fungal Allergen Elicits a Different Excitatory Synaptic Regulation Compared to Airborne Exposure to LPS in the Murine Brainstem Region Regulating Breathing

A Thesis submitted in partial satisfaction
of the requirements for the degree of

Master of Science

in

Biomedical Sciences

by

Sirajan Kamara

June 2023

Thesis Committee:
Dr. Monica J. Carson, Chairperson
Dr. Emma Wilson
Dr. Marcus Kaul

The Thesis of Sirajan Kamara is approved:

Committee Chairperson

University of California, Riverside

Dedication

This work is dedicated to my parents for teaching me everything from a young age until to this point. To my parents for letting me follow my instincts on pursuing this degree. I specially thank my mentor, Dr. Monica J. Carson for all her support, advice and believing me during this process. Without Paula Da Silva Frosts' mentorship and collaborator ship throughout this process it would be impossible, hence I also appreciate the guidance, thank you. Lastly, but not least, my best friend for life, Cindy Obregon for all the emotional and mental health support.

ABSTRACT OF THE THESIS

Airborne Exposure to Fungal Allergens Elicits a Different Excitatory Synaptic Regulation Compared to Airborne Exposure to LPS in the Murine Brainstem Region Regulating Breathing

by

Sirajan Kamara

Master of Science, Graduate Program in Biomedical Sciences
University of California, Riverside, June 2023
Dr. Monica J. Carson, Chairperson

We are using two modes of inflammation to trigger two different models of immune response: innate and adaptive immune responses. Using continuous exposure to aerosolized allergen, Alternaria *alternata*, triggers both innate and adaptive immunity, whereas using continuous aerosolized lipopolysaccharide (LPS) exposure triggers innate immunity only. Changes in the immunologic environment in the lung can communicate directly with the nucleus of the solitary tractus (NTS) in the medulla region. The response changes the synaptic plasticity among the neurons in NTS which may change physiological response of the breathing regulation under inflammatory conditions. Here, we are seeing how NTS changes its neuronal and glial cell plasticity as we expose mice to A. *alternata* (750μg/m^3) and LPS (1μg/m^3, 15μg/m^3). We are quantifying the presynaptic protein terminals and second messenger signaling cascade mechanisms of medulla region of C57BL/6J mice after seven days of allergic and bacterial particulates. For signaling cascade analysis, we are using GeoMx Digital Spatial Profiler (DSP), a multiplex technology that reads 96 targets using the nCounter technology and used five panels of protein contents for cell signaling pathways: Neuronal core proteins, Glial subtypes, Autophagy, PI3K-AKT and MAPK signaling. Data analysis shows a decrease of co-localized vglut2 and

synaptophysin puncta in A.*alternata* exposed females and an increase in higher dose LPS exposed females. There were no significant synaptic puncta co-localized regulation in neither exposed male mice. The protein analysis for the cascades shows different regulations of protein in both the exposed groups as well as between both sexes. In conclusion, the different models of inflammation suggest that female are having more synaptic regulation to the inflammations compared to males, however the signaling cascades remains differentially regulated and is sex specific.

Table of Contents:

List of Figures:

List of Abbreviations:

A.*alternata*	Alternaria Alternata
LPS	Lipopolysaccharide
NTS	Nucleus solitary tractus
PI3K-AKT	Phosphoinositide-3-kinase-protein kinase pathway
MAPK	Mitogen-activated protein kinase (MAPK)
BotC	Bötzinger complex
Pre-BotC	pre-Bötzinger complex
IgE	Immunoglobulin E antibodies
PAMP	pathogen associated molecular pattern.
APC	antigen-presenting cell
TLRs	Toll-like receptors
MHC II	Major histocompatibility class II
Vglut-2	vesicular glutamate transporters-2
EAAT2	Excitatory amino acid transporter-2
MERTK	MER Proto-Oncogene, Tyrosine Kinase
GPCRs	G-protein-coupled receptors
GSK3α/β	Glycogen synthase kinase-3 alpha/beta
AMPAR	α-amino-3-hydroxy-5-methyl-4-isoxazolepropionic acid receptors
NMDAR	*N*-methyl-D-aspartate receptor
S6K	ribosomal-6 protein kinase
IGF1	insulin-like growth factor-1

ERK	Extracellular signal-regulated kinase
MEK	Mitogen-activated protein kinase kinase
PSD95	Post-synaptic density protein 95
JNK	c-Jun N-terminal kinase
MyD88	Myeloid differentiation factor 88
TH	Tyrosine hydroxide
S100B	Calcium binding protein B
CD11b	α-chain of integrin receptor
CD11c	integrin alpha X
QC	quality check
SPF	specific pathogen free environment
PM	particulate matter
SEM	Standard error of the Mean
GeoMX DSP	GeoMX Digital Spatial Profiler
FOV	fields of view

Introduction:

Lung to Brainstem communication:

We are using bacterial and allergen aerosolized exposure paradigms to define how specific pathogenic attacks in lung, relay information to brainstem with the potential to modify the respiratory circuit regulating lung function. The lung during an inflammation sends sensory information directly to the nucleus of the solitary tractus (NTS) of the brainstem region. The bridge to this connection is through the vagus nerve that directly terminates in the NTS (Yackle, 2023). The intrapulmonary sites of the lung where most of the pathogen's insults taking place are innervated by nodose ganglion sensory neurons and are responsible to directly send signals to NTS (Yackle, 2023) (Hiroki et al., 2021). These neurons in the lung contain nociceptors that expresses toll-like receptors, for example toll-like receptor-4, which gets activated by the presence of lipopolysaccharide (Hiroki et al., 2021). Fc-epsilon receptors (FcεR1) are also present in the nodose ganglion that is activated in the presence of antibodies, such as IgE antibody, a common denominator of allergic airway inflammation (Hiroki et al., 2021) . The NTS then relays excitatory signaling information to the ventrolateral medullary regions: Bötzinger complex (BotC) and pre-Bötzinger (preBotC) complexes (Yackle, 2023). The pre-BotC region is responsible for controlling the inspirational phases of the lung as it transmits inspirational signals through the premotor neurons to generate diaphragm contraction of lungs (Yackle, 2023). The BotC region is responsible for the delay or inhibition of the pre-Botc activation of premotor neurons making the lung recoil for expiration (Yackle, 2023). For my project, I am analyzing how NTS changes its synaptic plasticity at neuronal junctions and communicates with these regions of the brainstem for breathing rhythm when we expose the mice to allergens and endotoxins in the form of aerosolized particulates.

Evidence of allergic response by Alternaria *alternata* in lungs:

Asthma, a common airway disorder, is easily triggered from various factors in the environment. Airway hypersensitivity is characterized by IgE immunoglobin mediated response in lungs (Holgate, 2008). Airways are sensitized in the presence of allergens such as house dust mite, pollens, ovalbumin and fungal exposures. Allergic inflammation is common among allergic diseases such as asthma, allergic rhinitis/rhinosinusitis, and atopic dermatitis (eczema). It is also important to understand that fungal exposures like A.*alternata* extract will recruit a robust innate and adaptive immune response with the presence of Immunoglobulin E (IgE) antibodies. Innate response is first triggered by the presence of pathogen infiltration. The pathogens have special pathogen associated molecular pattern (PAMPs) recognized by the macrophages. The macrophages have pattern recognition receptors such as Toll-like receptors that can recognize bacterial components. For examples TLR-4s PRR recognizes lipopolysaccharide, a component of gram-negative bacteria. The binding of PRR with PAMPs then trigger series of cytokines and interleukins which further activates other immune cells such as recruitment of neutrophiles as an innate inflammatory response. In the presence of an antigen, the initial immunity starts with the innate immune cell recruitments and then turns adaptive after a few days. The antigen-presenting cell (APC) and dendritic cells (DCs) engulfs antigens to aware the immunity of an adaptive response. The antigens present are then embedded in the major histocompatibility class II (MHC II) so that T- helper cells respond and release a series of cytokines. They also express two types of molecules $CD4^+$ or $CD8^+$ cells depending on the antigen present. The Th-2 $CD4^+$ type cells secrete interleukin-4 (IL-4), IL-5, IL-6, IL-13 cytokines than contribute to B-cells proliferation and isotype class IgE antibodies which also further recruits' eosinophils, an innate immune cell response (Holgate, 2008). Eosinophilic cells are the white blood cells that are commonly

recruited in the presence of allergic inflammation. The difference between a bacterial and allergen immune response is shown in figure 1. A. *alternata* is a common fungus, predominant in the outdoor mostly but studies have found these particulates to be very prevalent indoor as well. Fungal sensitivity is one of the most important factors of developing asthma and affects 24.6 million people in the United States (Knutsen et al., 2012). These aeroallergens are mostly present in environmental conditions like diurnal peaks mostly in areas with increase in CO2 and warmer weather, but they are also present mostly indoors with houses that are covered most in dust (Knutsen et al., 2012). Studies have shown that higher levels of A. *alternata* antigen in an area increases the odd of having asthma symptoms. Sato et al., have shown that the odd of asthma also increases in the location of one's home, and analyzed the kitchen room floor to contain the most antigen concentration versus bedroom bed containing the least antigen concentration (Salo et al., 2006). The antigens of A.*alternata* causes a trigger to long-term adaptive immunity in lung, however, how this immunity pursued is still unknown, which is why we are studying the synaptic regulation in the NTS region under the influence to aerosolized A.*alternata*.

Why we chose Aerosolized A.*alternata* exposure:

Average household consist of 4.88 ug/g of A.*alternata* concentration for people to have a IgE-mediated hypersensitivity (Salo et al., 2006). To further gain our knowledge on fungal particulate allergen sensitization in brainstem, we used an environmental chamber in which mice were maintained in their usual husbandry cages (Peng et al. 2018). The entire cage was placed in the chamber, allowing mice to maintain their familiar environment, without restrictions on their movement and giving them the usual access to food and water. Using this chamber, mice were exposed for 7 days to aerosolized noninfectious A. *alternata* particulate extracts (750 ug/m^3). This exposure paradigm has been demonstrated to trigger both innate and adaptive immunity

through the recruitment of immune cells found in lavage collection (Peng et. Al 2018, Biddle et al. 2021). The neutrophils are the first cells recruited, within the first six hours, to provide an innate immune defense. Biddle et al. have shown an increase in T cell and eosinophil recruitments using this exposure route; proving the presence of adaptive inflammation seven days after this exposure (Biddle et al., 2021). Other studies have been exposing through different types of deliveries of this particulate such as through intraperitoneally, intranasally or through primary human/ mouse airway epithelial cells. Hee-Kyoo et al used intranasal A.*alternata* extract and have shown Th2 helper cell recruitment (Kim et al., 2014). The different methods of A. *alternata* instillation have shown similar response to this particulate. Our studies have also compared both route of instillation of A.*alternata* intranasal and aerosolized, they have seen that aerosolized exposure was sufficient and had 60% increase of immune cell recruitments in lung compared to intranasal dosage (Peng et al., 2018). This shows that aerosolized chamber exposure was sufficient to trigger both innate and adaptive allergic immune response in lungs and a well characterized system that demonstrate in vivo health studies regards to air pollutants in the environment. As a result, we decided to further examine the brainstem regulation under this exposure route.

Lipopolysaccharide:

The A.*alternata* extract is a complex mixture triggering a polarized allergic inflammation. Here I am using lipopolysaccharide (LPS), a potential innate immune activator, as a contrast experiment to A.*alternata* exposure and to determine whether NTS will respond similarly regardless of the type of exposure and the type of inflammation triggered. LPS is a component of a gram-negative bacterial organism. This bacterium has two membrane layers the inner and outer membranes (Bertani & Ruiz, 2018). The outer membrane of this bacteria contains

phospholipid lining the inside and lipopolysaccharide molecules lining on the outer side of the membrane. These molecules not only make the layer an effective permeable barrier from small hydrophobic molecules but also creates an important role in bacteria-host interactions (Bertani & Ruiz, 2018). The LPS glycolipid itself has two components which are lipid A, core oligosaccharide and the O antigen. Lipid A is at the outside layer of the membrane which is hydrophobic made of glucosamines (Bertani & Ruiz, 2018). The O antigen layers are attached to the oligosaccharides with two to eight sugars. The lipid A component of LPS is what the host toll-like receptors 4 (TLR-4) recognizes (Bertani & Ruiz, 2018). LPS administration is a consistent model of innate immune inflammation, and its inflammatory response have been characterized and reproduced by many groups. Its recognition generates tumor necrosis factor (TNF)-alpha, interleukin (IL)-1b, IL-6, a similar response to active bacterial infection, but non-replicating and short lived (Martin et al., 2013). Here, we are delivering LPS the similar as A. *alternata* to study brainstem alterations. Common modes of LPS delivery such as intranasal, and intraperitoneal are also known to elicit brainstem alterations. G. Gakis et al., have induced NTS sensitization through LPS by injecting it interperitoneally and Kannan et al., also successfully triggered LPS endotoxin inflammation in the brainstem of rat pups through intratracheal instillation (Gakis et al., 2009) (Balan et al., 2011). However, for my project, I am utilizing an aerosolized delivery of LPS 1μg/m^3 and 15 μg/m^3 dosage to assess how the innate inflammation in lung is transmitting immune signals in the NTS of the brainstem through analysis of protein regulation in intracellular neuronal signaling of brainstem and comparing it to A.*alternata* exposure data. Biddle and colleagues (2021) have previously demonstrated that airborne exposure to LPS for 1 week (LPS 1μg/m^3) does trigger lung inflammation but the inflammation is transient, dominated by neutrophilia with a paucity of eosinophils and lymphocytes. Therefore, it is an ideal exposure to test my hypothesis that the NTS will have exposure-specific responses.

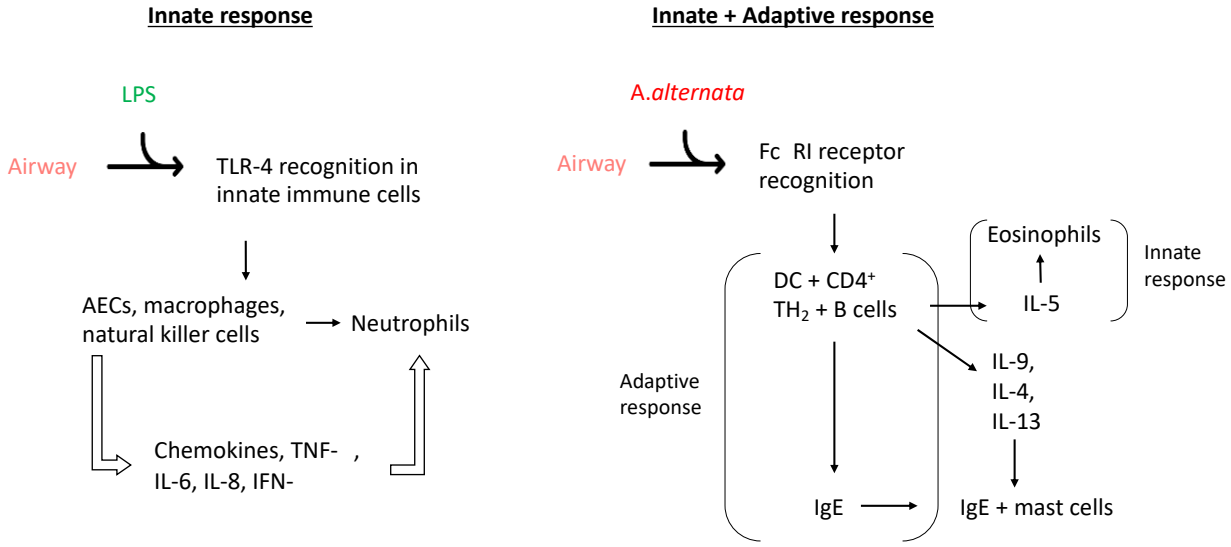

Figure 1: Innate and adaptive response from different exposures.

Lipopolysaccharide (LPS) elicits an innate response when toll-like receptor 4 (TLR-4) recognized the LPS component. These receptors are on Airway epithelial cells (AECs), Dendritic cells (DCs), macrophages which recognizes the component. These cells then release chemokine, series of interleukins such as IL-6, IL-8, tumor necrosis factors alpha (TNF-α) which then contributes to recruitment of neutrophils from blood capillaries causing an innate inflammation. Allergens like A.*alternata*, elicits not only an innate response but also an adaptive response. The DCs, T-helper cells TH_2 cells and B cells bear allergens presentation inside and makes immunoglobin E (IgE) productions with the help of major histocompatibility class II (MHC II). They also release interleukins such as IL-5, which helps recruit innate immune cells such as eosinophils, a characteristic for allergic inflammation.

Synaptic plasticity at Medulla:

Synaptic plasticity is the changes within synapse junctions that occurs so that neurons can communicate with other neurons in different regions of the brain. We have exposed A.*alternata* and LPS in our C57BL/6J mice to induce changes in the medulla region of the brain because of the direct communication of lung's innate and adaptive immunity through vagus nerve. The communication in the Nucleus of the Solitary Tract (NTS) of the medulla region will respond to the particles/pathogen insults in lung and physiologically communicate with other regions of the medulla through a very fine regulation of synaptic coordination (Kline, 2008). Here, we wanted to see this coordination as they change synaptic plasticity at the synapse junction between neurons to neuron communication. Since glutamate is a major excitatory neurotransmitter among neurons and has major roles in synapse induction, elimination, and neuron-to-glial communication. Therefore, we are using pre-synaptic vesicular glutamate transporters-2 (vglut-2) and synaptophysin markers to identify their interaction for glutamate releases after A. *alternata* and LPS exposure mice in neuron terminals. Vglut-2 are major transporters responsible for up taking glutamate into the vesicle of the pre-synaptic terminals waiting to be released once depolarized. Synaptophysin takes a major role in docking the vesicles with the presynaptic terminals to release the neurotransmitters. The formation of synaptobrevin and synaptophysin is to provide a template to assemble the proteins responsible for exocytosis of the neurotransmitters (White & Stowell, 2021). It is important to maintain the glutamate levels both inside the neurons, glial cells and in the synaptic cleft once the glutamate is being released from the synaptic vesicles. Glial cells take part in clearing of glutamate by up taking these neurotransmitters through their own glutamate transporters. Excitatory amino acid transporter-2 (EAAT2) is a major glutamate transporter in astrocytes to assess the clearance of glutamate. Once taken in, glutamate undergoes glutamate metabolism and releases the glutamine precursors back to the

neurons as a means to recycle the neurotransmitters (Mahmoud et al., 2019). This way astrocytes contributes to the glutamate homeostasis in CNS at a physiological condition. Microglia is an important glial cell to keep the microenvironment of the CNS to be healthy. Its core properties include surveillance, phagocytosis and release of soluble factors when needed (Paolicelli et al., 2022). It is imperative to understand that microglia are always active and sensing its environment and always homeostatic during physiological state (Paolicelli et al., 2022). However, while homeostatic it has different morphological and homeostatic functions depending on CNS microenvironment and it's specificity is identified by the markers expressed (Paolicelli et al., 2022). For example, MerTK, a TAM tyrosine kinase receptor in the surface of the microglia is responsible of phagocytic clearance of synaptic pruning in a homeostatic condition. At a physiological condition, the phosphatidylserine (PS) is a phospholipid is released by neurons at the outer member from inside by type IV P-type adenosine triphosphatases (P4-ATPases) which requires flippase chaperone cell cycle control protein 50A (Cdc50a) activation (Park et al., 2021). Stressed neurons releases PS with the help of Cdc50a to activate MerTK receptors of microglia (Park et al., 2021). On the other hand, expression of $CD11b^+$ and $CD11c^+$ identified for dendritic cells are responsible for surveillance but also detects T cell interactions in the lymph tissue in the presence of MHCI/MHCII classes (Colton, 2013). These cells are usually found in the choroid plexus and ventricles of the brain region due to the close proximity of cerebral spinal fluid where presence of antigens are found (Carson et al., 2006; Colton, 2013). Lastly, administrations of pathogenic insults affects the physiological mode of excitatory glutamatergic neurotransmissions. Such as Mascarucci et al., have found that intraperitoneal injections of lipopolysaccharides have increased the release of glutamate into the synaptic cleft than through intravenously (Mascarucci et al., 1998). Since the model of LPS delivery does affect the release of glutamate, we wanted to use our chamber exposure to best fit environment like humans and characterize patterns of

membrane glutamate protein transporters in the synaptic terminals to make sense of how glutamate is being regulated.

Neuronal second messenger signaling cascades:

The binding of the glutamate to the glutamate receptors whether its glial or neuronal terminals, then triggers second messenger intracellular signaling pathways. The second messenger intracellular signal is affected through activation of second messengers and protein kinases. G-protein-coupled (GPCRs) then comes into play by changing its confirmation and along with beta-arrestins then signals mitogen-activated kinases (MAPK), phosphoinositide 3-kinase (PI3K) and autophagy cascades. These signaling pathways are believed to regulate downstream signaling of proteins responsible of glial, neuron morphology and synaptic plasticity.

PI3K-Akt Pathway:

Phosphoinositide 3-kinases (PI3Ks) is an integral element that triggers the PI3K-AKT pathway signaling promoting cell metabolism, cell survival, growth and autophagy from stressful environments. There are many key molecules that triggers this signaling however some of the important receptors involved includes tyrosine kinase (RTKs), phosphatidylinositol 3-kinase (PI3K), phosphatidylinositol-4,5-bisphosphate (PIP2), phosphatidylinositol-3,4,5-bisphosphate (PIP3) and AKT/protein kinase B (Long et al., 2021). They are also activated by GTP binding RAS protein. The binding of Akt protein through mTORC2 will trigger AKT signaling activity (Ersahin et al., 2015). This binding is important in activation or suppression of many other proteins in this pathway. For example, Akt phosphorylates GSK3 isoforms therefore inactivates the kinase which is for regulation of apoptosis and glucose metabolism. GSK3 has many roles but in the means for neuronal regulation, activation of this protein, specially GSK3β isoform, have

shown to inhibit presynaptic vesicle exocytosis by dysregulation of synaptophysin with the presynaptic membrane proteins therefore, decreases the release of glutamate (Zhu et al., 2010). They have role in regulation of AMPAR and NMDAR regulation in controlling the long-term potential plasticity in hippocampus (Wei et al., 2010) (Liu et al., 2017). Similarly, the PI3K-AKT pathway also have a protective neuronal affect from many apoptotic stimuli, under many neurological diseases. AKT also indirectly activates mTORC1 signaling which is major component of cell growth. Along with this, AKT also activates ribosomal protein S6 kinase (S6K) which then phosphorylates ribosomal S6 to promote the cell growth. This pathway is also known to play a significant role in glutamate transmission uptake in synaptic terminals. The uptake of the neurotransmitter requires energy since there are ion pumps, trafficking and signaling pathway requirement, however, is important to modulate the energy use. Glucose metabolism in brain is important for ion pumping and glutamate synthesis for example in glial cells. Insulin being a key signaling factor in responding to this pathway encourages glucose uptake. In the presence of insulin and insulin-like growth factor-1 (IGF1) binds to receptor tyrosine kinases that is an upstream activator of PI3K-AKT pathway in aged hippocampus (Amato & Man, 2011). The presence of both IGF1 and AMPK helps translocation of glutamate transporters in the neuronal membranes (Amato & Man, 2011) However, PI3K-AKT pathway's role to regulate synaptic plasticity in the NTS under innate and adaptive inflammation is still unclear.

MAPK-ERK1/2 pathway:

Mitogen activated protein kinases pathway plays similar role of cellular proliferations, growth, differentiation, migration, and death. Activation of MAPKs then leads to mediation of many phosphorylated kinases. These pathways also activate phosphorylated kinases such as

ERK1 and ERK2. ERK1 and ERK2 (p44 and p42 MAPK) also have an important role in mature neuron and their synaptic plasticity. In the presence of growth factors and other stimuli, the hydrolysis of GDP to GTP by Ras triggers Raf that phosphorylates and activates enzyme MAPK/ERK kinase (MEK) which then activates ERK1/ERK2 kinases (Rosen et al., 1994). The binding of RAS for MAPK signaling kinase also is responsible for AMPA-R trafficking and removal to regulate excitatory glutamatergic transmission (Qin et al., 2005) . This pathway is also triggered by glutamatergic signaling as there is a calcium influx inside the terminals with the help of NMDA or voltage gated CA+ channels. Cells that are undergoing stress activate JNKs (stress-activated kinases), c-Jun being the substrates of JNK and when phosphorylated leads to cell apoptosis, differentiation, and proliferation. JNKs along with activation of JNK-interacting protein 1 (JIP1) scaffold protein helps decrease synaptic plasticity as they regulate NMDAR type glutamate signaling and PSD95 recruitment in hippocampal region (Morel et al., 2018). This pathway is stimulated by the excitatory glutamate regulation within neuronal terminal hence it is important to understand the role of this cascade in the presence of lung inflammation and how it is being regulated through the synaptic changes in NTS.

Autophagy:

Autophagy is known to reduce pathogenic attacks by degrading and destroying neuronal debris. For example, in the presence of LPS as the TLR4 is activated alongside MyD88 a canonical adaptor for signaling pathways downstream of TLRs that further activates TIR-domain-containing adaptor proteins to activate autophagy (Cadwell, 2016). They then release beclin-1, transcription of LC3-binding proteins for autophagosomes, such as sequestosome 1 (SQSTM1), optineurin (OPTN) and NDP52. Autophagosomes are responsible for recognition of damaged pathogen vesicles like LPS and prevents its activation (Cadwell, 2016). Similarly for fungal

glycans and immune complexes, the Fcγ receptor (FcγR) activates the LC3-associated phagocytosis (LAP) and acidifies the fungal complexes (Cadwell, 2016). Autophagy is also activated in response to neurotoxicity, hence important to modulate synaptic plasticity and neuronal survival when triggered. This pathway is also responsible for regulating integrity of synaptic vesicle at post synaptic sites as well. The way this pathway regulates synaptic plasticity is by degradation of some post synaptic scaffolding proteins for example, PSD-95, SHANK3 and PICK1 (Hwang et al., 2019). Inhibition of this pathway have had an increased expression of these scaffolding proteins. Autophagy has been documented with addictive and neurotoxic drug abuse such as methamphetamine (METH) and how the drug manipulates and causes dysfunction of protein regulations related to this pathway (Hwang et al., 2019; Limanaqi et al., 2021) .

Using a high-plex spatial profiling instrument, GeoMX, will gives us a platform to analyze more than ninety-six proteins involved in the signaling cascades stated above to identify how neurons are controlling the intercellular signaling under the influence of two different types of exposure.

Sex specific effect:

For us to see a sex-specific effect, we have used equal number of males and female mice for our exposures. It is imperative to show an equal representation of both the sexes as the new research emerges in this era. Females are different from males through the definition of sex chromosomes. The SRY gene being the sole provider of region with sex-determining protein Y, for male character development and for the development of male gonads during fetus stage. The females have two X chromosomes, XX, making them unique from males because of the absence of SRY genes. The genetic make-up of both the sexes also contributes to the immunity of innate

and adaptive inflammation. Males with Klinefelter syndrome, an extra X, have an immune system similar to females with an increase in CD4/CD8 T cell ratios compared to their control male groups and females with Turner syndrome, only one X, have lower IgG and IgM levels compared to the control females (Klein & Flanagan, 2016). Hence it is important to take both males and females into consideration since they have a differential regulation of innate and adaptive immune response, where females have higher $CD4^+$ T cells counts and males express more $CD8^+$ T cells (Klein & Flanagan, 2016). The X chromosome have many genes involved in the higher innate immune response, for example TLR7, which is responsible for IFN-alpha for virus detection (Jaillon et al., 2019). Studies have also found that the dosage of the X-chromosome contributes to the TLR7 production and increases with higher X chromosomes (Jaillon et al., 2019). Hence females with two X chromosomes will tend to have a higher innate response than males since they have only one X chromosome in the pair. Studies have also found that brain injury under a hypoxia insult have shown that females elicit a different stronger apoptotic response than males. Caspase-3 activation, an upstream signaling of cell death, was more pronounced in female neurons whereas males showed translocation of apoptosis inducing factors (AIF) mainly because of XX neurons versus XY neurons (Zhu et al., 2006). As a result, to see if there is a sex difference in the NTS region of the brainstem of both sexes we were able to analyze both females and males separately to show the differential regulation of the immune response at the neuronal synaptic level.

Methods and Material:

Wild-type mouse model:

Under the University of California Institutional Animal Care, adult C57BL/6J mice were maintained with fresh bedding and standard Purina food chow in Vivarium for each of the experiments under specific pathogen free environment (SPF) until the time of experiment. We used six males and females for the A.*alternata* exposure and control groups. We used three males and females for LPS exposure and their control groups.

Chamber exposure

Mice were exposed treatments in environmental exposure chambers as previously described (Peng et al. 2018, Biddle et al. 2021). The exposure chambers include dual 540 L chambers for control (air) and experimental (LPS and A.*alternata*). The internal environment was measured consistently by monitoring the levels of humidity, temperature, atmospheric pressure and ammonia for selective experimental exposures. To ensure zero light contamination, the chamber was covered with black cloth. The experimental chamber fed mice with dry filtered air (0.5-1 lpm) and aerosolized spray where the selected particulate matter (PM) was dried by two in-line silica gel columns, (3.5-4.5 lpm). The particulate matter was collected from Alternaria *alternata* and Alternaria *tenuis* filtrate (Greer Laboratories, Lenoir, NC, USA; 0.4 g/L) and Lipopolysaccharide (LPS) from Escherichia coli O55:B5 (Sigma Aldrich, St. Louis, USA). The mice in the control chamber only had filtered dry air (5.0 lpm) compared to experiment and kept every condition the same which includes: bedding replacement, food, water cycle and day/night cycle. The concentration used for each particulate matter for the experimental chamber were: 1 $\mu g/m^3$, 15 $\mu g/m^3$ for LPS and 750 $\mu g/m^3$ for A.*alternata* evenly atomized and distributed in the chamber for seven days.

Animal processing:

After 7 days of exposure, mice were collected from the chambers then euthanized using isoflurane. The whole brain was perfused using 20 ml PBS and 20 ml of 4% PFS. They were then submerged in 4 % PFA for 24 hours, following in PBS/30% sucrose solution for 48 hours. The brains were then dissected for brainstem and mounted in OCT separately for brainstem regions. The dissected sections were OCT preserved in -80 degrees for immunofluorescent (IF), imaging and GeoMX experimental procedures.

Western blot analysis

Isolated medulla samples were centrifuged at 12,000 x g, 4°C, for 20 min, and pellets were resuspended in RIPA lysis buffer (89900, Thermo Fischer) containing 100X protease inhibitor cocktail (P8340, Sigma Millipore), EDTA and phosphatase inhibitor phosSTOP (04906837001, SigmaAldrich) and incubated for 2 h at 4°C. Samples were added to 5x Lammeli Buffer and run on an 12% Acrylamide gel. Protein samples were transferred onto a nitrocellulose blotting membrane. Blots were blocked with 3% milk in TBS, followed by immunostaining with EAAT2 antibodies (22515-1-AP) in 0.1% Tween 20 in TBS at 4°C for 16 h. Secondary antibodies used were donkey anti-rabbit 546 (A11035, Thermo Fischer). Membranes were imaged on ChemiDoc™ MP imaging system (BIORAD). Band density was analyzed by measuring band and background intensity using Image J.

Immunofluorescent staining (IF)

Brainstem tissues were cryopreserved and cryosectioned at (5µm and 20µm) coronal sections of medulla for IF staining. The sections collected were bregma -7.64mm for NTS, bregma -6.64 for PreBotC and -6.84mm for BotC. The tissues were then placed on the plus side of the Fisher

scientific super frost microscope slides. They were stained with guinea pig anti- Vglut2 (AB2251-I), and mouse anti-synaptophysin (AB8049) along with their conjugated secondary anti-bodies Alexa-647 anti-goat guinea pig (A21450) , and Alexa-488 anti-goat mouse (A11029). The tissues were stained with Prolong gold containing Dapi for nuclear staining and mounted ready for Yokogawa spinning disc confocal microscopy system for imagining.

Western blot and Puncta quantification:

Using a confocal microscope, NTS synaptic puncta was imaged at 63X objective using confocal microscope system and three images were taken to represent the region. For the analysis of vglut2, synaptophysin, and their colocalization of each puncta, I used Nguyen et al. analysis where each image is threshold-adjusted to (0-160 intensity) and puncta numbers (0.5-10 um^2) were collected using the NIH ImageJ software (Nguyen et al., 2020). Colocalization of vglut2/synaptophysin and vglut2/PSD95 were then analyzed by ImageJ plugin for colocalization (https:// imagej.nih.gov/ij/plugins/colocalization.html).

Statistics:

Puncta analysis

For Puncta quantification, statistical analysis was performed using two-way ANOVA along with Tukey post hoc analysis/ unpaired t-test in GraphPad prism software version 7. For western blot analysis, statistical analysis was performed using unpaired t -test using GraphPad Prism 7 software (RRID: SCR_002798). Data represent Mean +/- SEM.

Western blot

Statistical analysis was performed with unpaired t test using GraphPad Prism 7 software (RRID: SCR_002798). Data represent mean +/- SEM.

GeoMX DSP:

GeoMX Digital Spatial Profiler (DSP) is used for high-plex digital quantification of proteins by using part of standard immunofluorescent technology with nCounter barcoding protein quantification. The tissue samples are collected by 5um thick and mounted in Superfrost Plus slides and making sure the samples are mounted in the center of the slide no further than 35.3mm long by 14.1 mm wide.

Day 1

For the antigen retrieval step, we used a 1x citrate buffer at high pressure and high temperature in a pressure cooker for 15 minutes. After letting it stand for 25 mins to cool the slides with samples. The blocking is attained by using Buffer W solution for 1 hour inside the humidity chamber. For the antibodies, we need a total volume of 800µl of working antibody mix solution for each slide with 32µl of each morphology marker used and 1.6µl of the TH antibodies in the antibody mix with the remaining solution of Buffer W. The antibodies used are TH (Tyrosine hydroxide) to characterize the NTS neurons for visualization and morphology markers that contain antibodies from the five panels we chose for asking our research questions. We are using morphology markers from neuronal core mix, glial subtypes, autophagy, PI3K-Akt and MAPK signaling also shown in Figure 1. The diluted antibody solution is then applied to each slide with 200ul of the solution in the humidity chamber. This is then placed in the 4-degree Celsius refrigerator overnight.

Day 2

This day starts with post post-fixation step with 4% PFA of 200ul for each slide in room temperature for 30 minutes. To stain our samples with a nuclear stain, we used SYTO 13 at 1:10 dilution with TBS1x and stained 15 minutes for 200µl for each slide. The stained slides can then be stored at TBS-T until loaded to the DSP machine.

The slides are then placed in the slide holder facing up where the samples are and 6ml of the Buffer S is added. The slide holder of the DSP machine can only hold four slides each run so we can only run 3 samples of each air and experimental group at a time. We then place a collection plate where the samples from the slides will be aspirated and collected on to. The next step is preceded by identifying the slides in the system by selecting the morphological reagent kits used to stain and entering the lot numbers provided by the company. The focus channel is selected for FITC/525 nm for the SYTO 13 staining and Texas Red 594 nm for TH neuron staining to have a better visualization when selecting our region of interest (ROIs). The region of interest for our experiment is the NTS and is selected using a custom polygonal button from the DSP's scan workplace. Once the ROI is approved, the DSP will start the collection of the oligos attached to the antibodies. The UV light will shine to the selected region of interest and in our case, the NTS region, and the cleaved tags from the region are collected onto a microplate well. The plate is then collected and sealed with semi-permeable membrane and incubated at 65 degrees Celsius for 1 hour in a thermocycler to dry down the aspirate samples. For the nCounter machine to count the proteins collected from ROIs, we use hybridization codes that bind to the nucleic acid targets. We have Probe R that binds to the reportage tag of the specified nucleic acid target and Probe U that binds to its universal capture tag. The master mix of 84μL (Probe R + Probe U and Hybridization buffer) is created and added to the hybridization codes solution based on the rows of the microplate the aspirated samples are collected onto by the DSP. The mixes are then added to each well for 8μl and incubated at 67 degrees Celsius in the thermos cycler for 16 hours.

Day 3:

Once the plate is at the 4 degrees Celsius, the products are pooled into a 12 strip tubes and the concentration pooled are based on the segment area of ROI collected from the lab worksheet the

DSP provides at the end of the experiment in day 2. The pooled samples are then loaded to the sprint cartridge with 30µl of sample volume and then submitted to the nCounter machine ready to quantify the protein expressions. The reporter code count (RCC) files are then obtained.

GeoMX analysis:

To analyze the RCC files, I used the GeoMx data analysis suite website. The data first goes through quality check (QC) to evaluate the quality of the samples. The parameters include fields of view (FOV) of 75% to make sure to obtain a robust data. The binding density of 0.1-1.8 to make sure the nCounter detects the barcodes per square microns. For data normalization, the data is either normalized by positive control proteins (GAPDH, S6 and H3) or negative control (Rb IgG, Rt IgG2a and Rt IgG2b) by running a correlation plot between each of the protein (Figure 2A,3A,4A). After either choosing the positive or the negative controls, their geometric mean is used for normalization, producing a normalized value with every protein of each sample. The normalized value of each protein is transformed to logarithmic base 2 value and is graphed (Figure 2B,3B,4B). Any proteins below the zero value are excluded as listed below. In the DSP, the proteins are excluded and the volcano plot is generated by Log 2 fold change (x-axis) and -log10(adj.p-value) (y-axis) using the linear mixed model and Benjamini- Hochberg method.

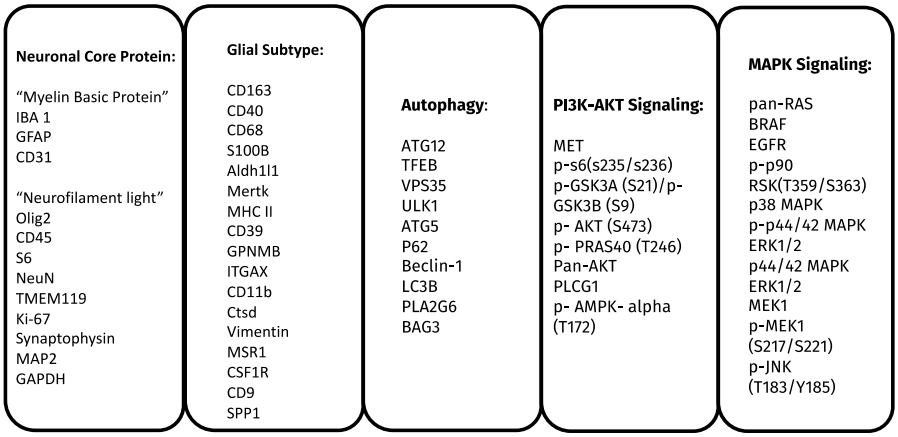

Figure 2: Antibodies analyzed from each panel for GeoMX.

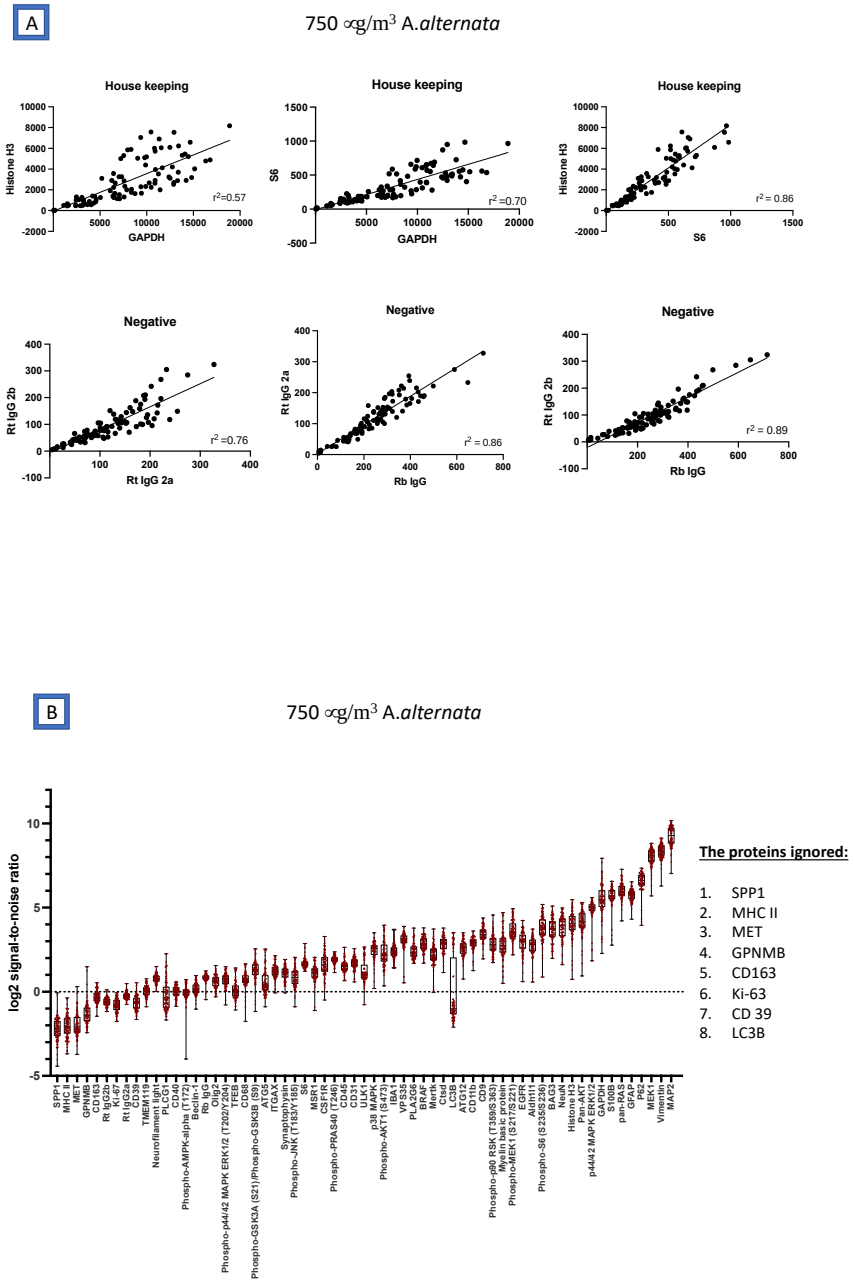

Figure 3: (A) Correlation between the positive protein and negative protein for data normalization. (B) represents logarithmic base 2 protein value to exclude proteins for analyses.

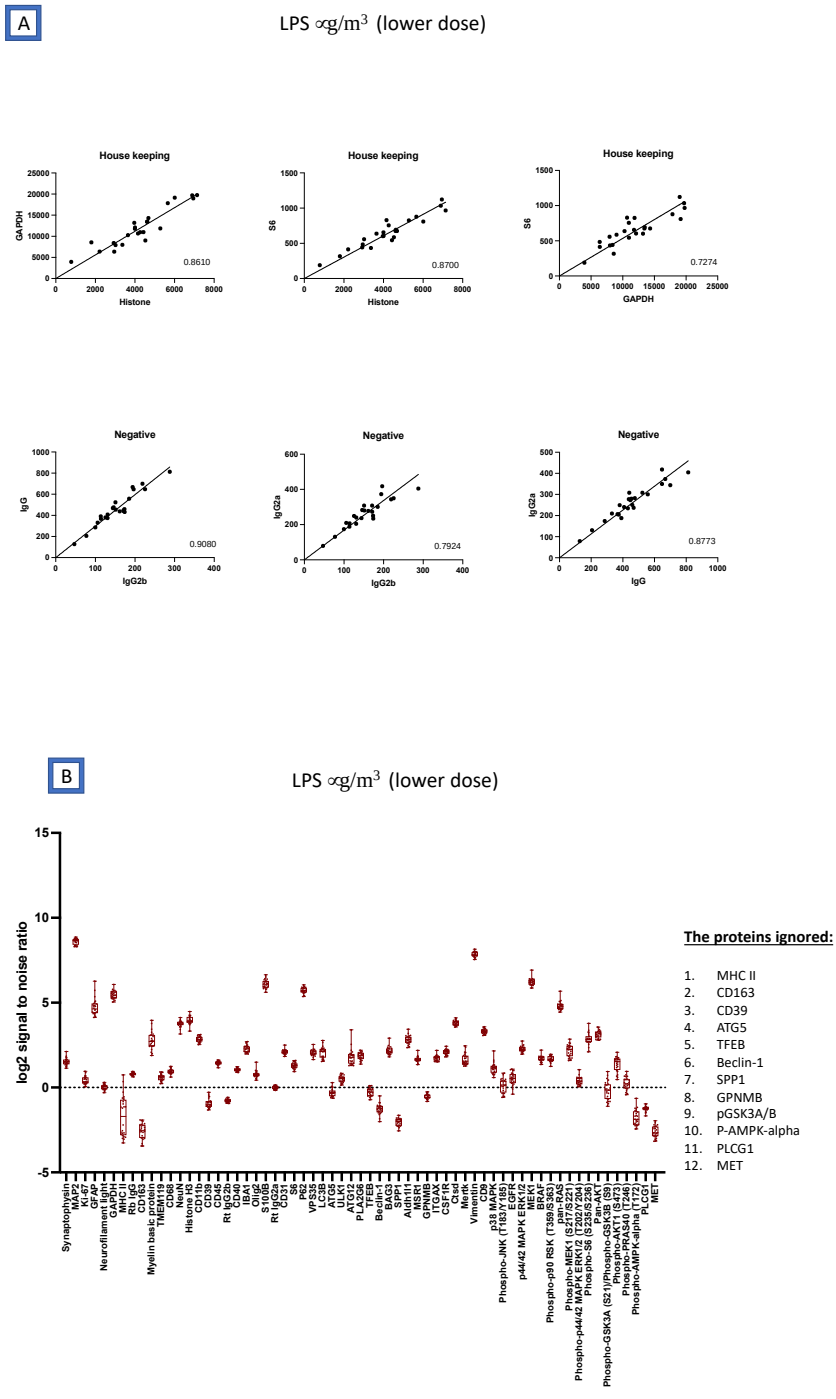

Figure 4: For 1ug/m^3 (lower dose) (A) Correlation between the positive protein and negative protein for data normalization. (B) represents logarithmic base 2 protein value to exclude proteins for analyze.

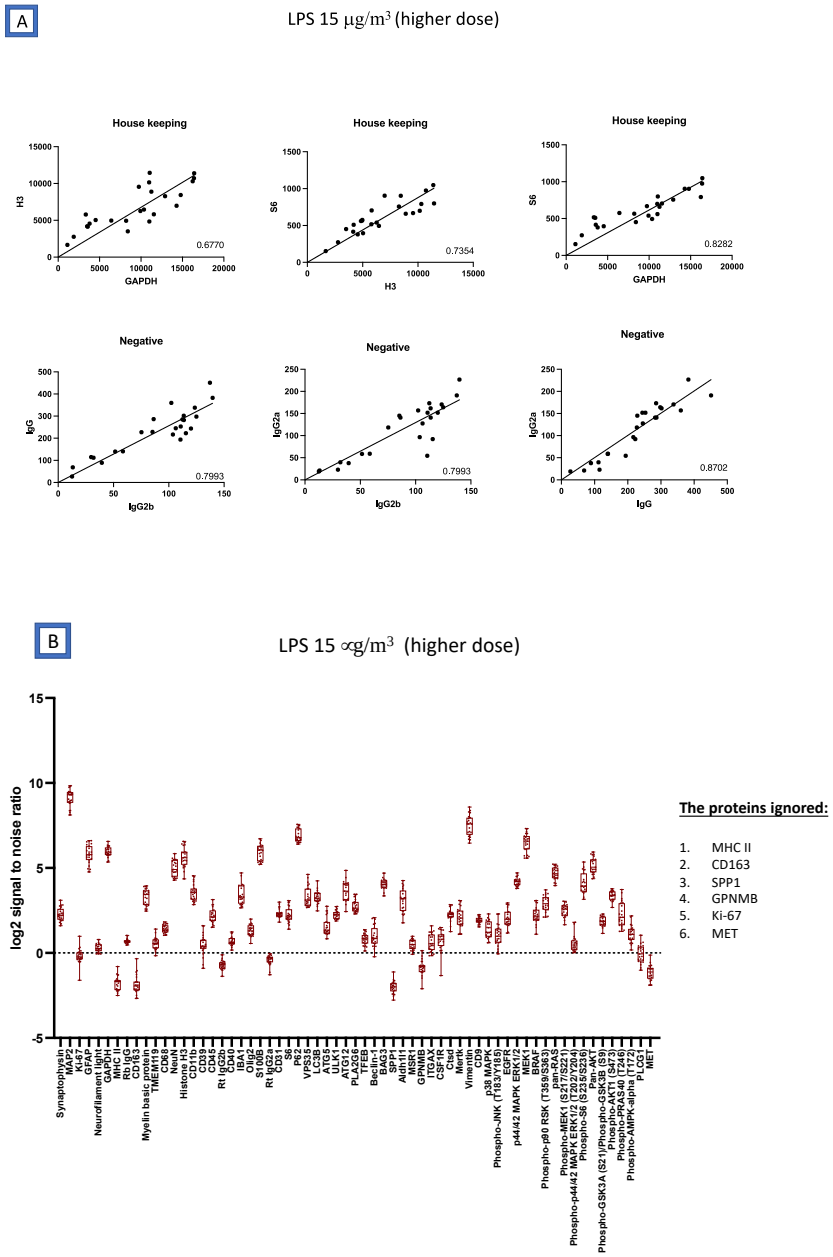

Figure 5: For 15 ug/m^3 (lower dose) (A) Correlation between the positive protein and negative protein for data normalization. (B) represents logarithmic base 2 protein value to exclude proteins for analyses.

Results:

Synaptic regulation in Nuclei of the solitary tract (NTS) by Alternaria *alternata*

The Brainstem which includes the NTS region was collected from adult female and male mice after the 7-day A.*alternata* aerosolized chamber exposure. For Figure 6, we have stained the NTS region of the brain with vglut2, and synaptophysin antibodies since we wanted to observe how the glutamate vesicles synapsing in the neuronal terminals to release the neurotransmitters. Based on the quantification, we saw there were no changes in the puncta numbers of vglut2 and synaptophysin for exposed females (figure 6D,E) and males' figure (6J,K). However, the data shows a decrease in co-localized puncta of vglut2 and synaptophysin numbers in exposed females (Figure 5F) when compared to the control females shown in figure 6C. Upon performing the analysis, males did not show a profound affect in any puncta quantification (figure 6I, J), concluding that females respond more to regulation of the allergic inflammation and a sex-specific effect is observed only in females.

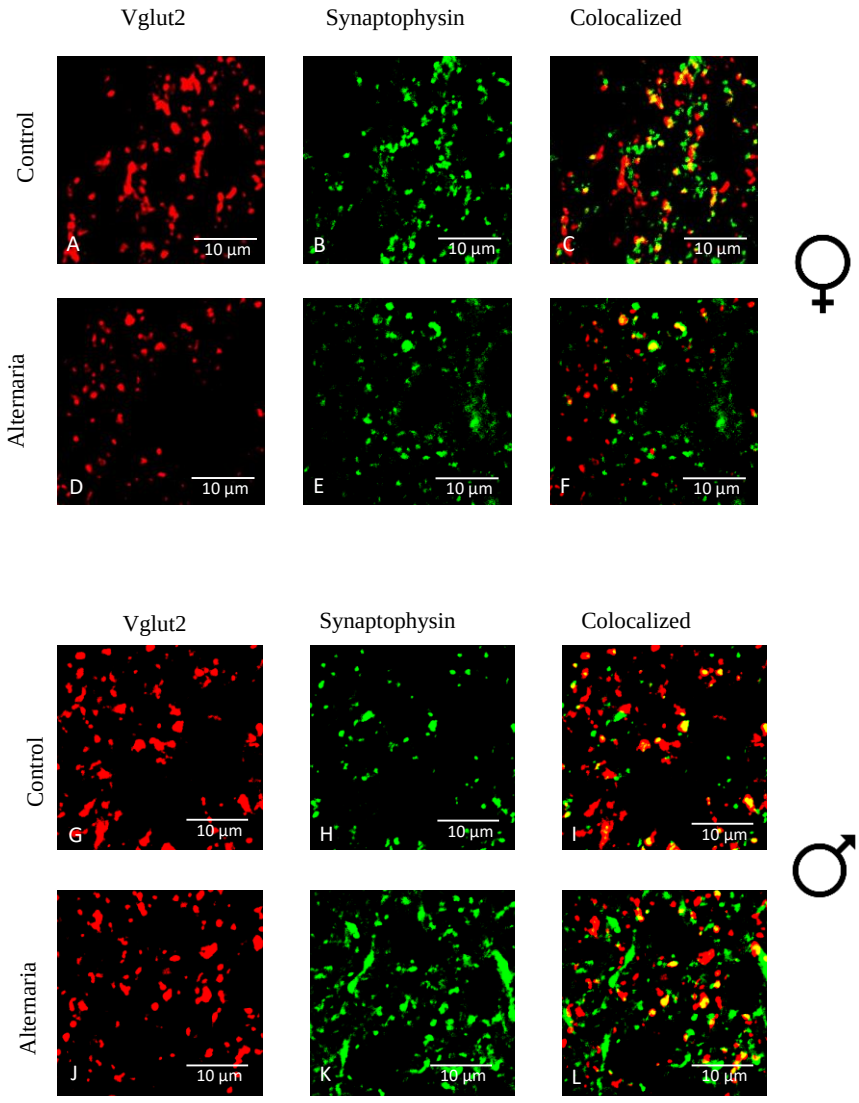
Vglut2
Synaptophysin
Colocalized
Control
Alternaria
A
B
C
D
E
F
G
H
I
J
K
L
10 µm
♀
♂

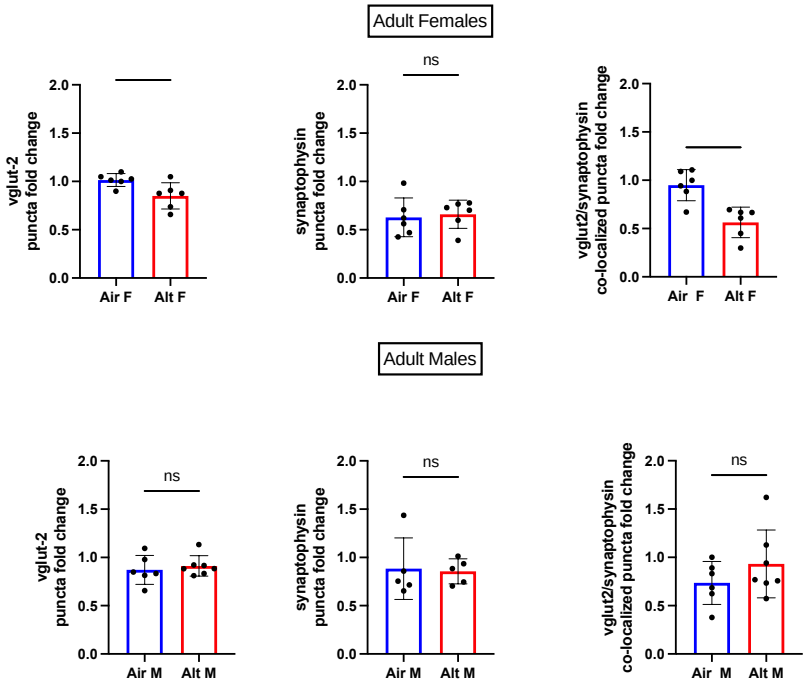

Figure 6: Sex difference in NTS regions of mice.

The images (A-L) are stained with Vglut-2 and synaptophysin at NTS region of medulla at 63x. (A-C, G-I) is air chamber exposed mice females and males (N= 6 biological sample, n= 3 technical replicates), (D-F, J-L) is A.*alternata* chamber exposure female and male mice (N= 6 biological sample, n= 3 technical replicates). Puncta for colocalization, vglut-2 and synaptophysin were calculated for these images. For females, the colocalization value is p = 0.0260*, vglut2 is p = 0.2855, synaptophysin is p = 0.8754. For males, the colocalization is p= 0.2560, vglut2 is p = 0.3816 and synaptophysin is p = 0.2237.

Synaptic regulation in the Pre- botzinger and botzinger complexes.

The ventrolateral medulla regions: Pre-botzinger and Botzinger regions of adult female and male mice were collected after the 7-day aerosolized A.*alternata* exposure. We hypothesized that seeing a decrease in synaptic regulation in A.*alternata* exposed females of NTS region of the medulla would then further project to PreBotC and BotC complex to regulate respiratory rhythm and pattern formation. The data shows no significant differences in the puncta levels of vglut-2, synaptophysin and colocalization of both sexes in the PreBotC region as shown in Figure 7. Next quantifying the puncta numbers of vglut2, synaptophysin and co-localization of both sexes showed no pronounced difference in the region BotC compared to their control either shown in Figure 8. This indicates that there is no significant puncta regulation and excitatory synaptic input from the NTS region to regulate glutamate in presynaptic levels at the 7^{th} -day of adaptive inflammation.

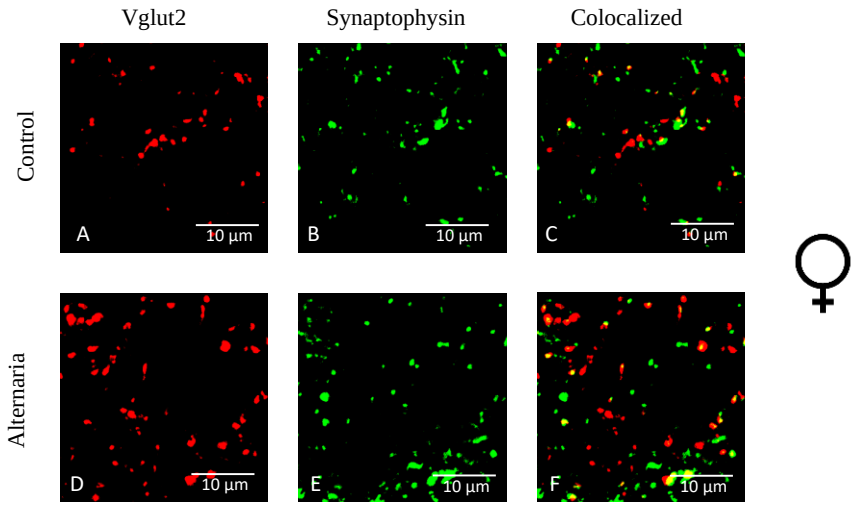
Vglut2
Synaptophysin
Colocalized
Control
Alternaria
A
B
C
D
E
F
10 µm

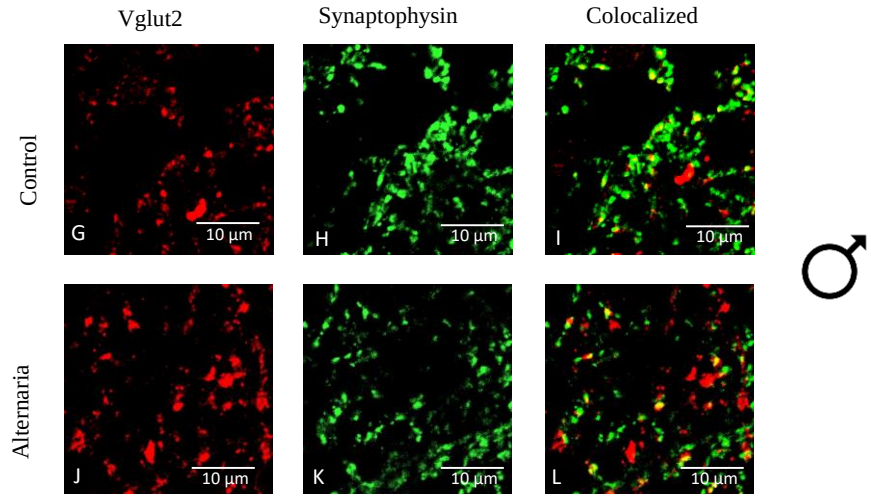
Vglut2
Synaptophysin
Colocalized
Control
Alternaria
G
H
I
J
K
L
10 µm

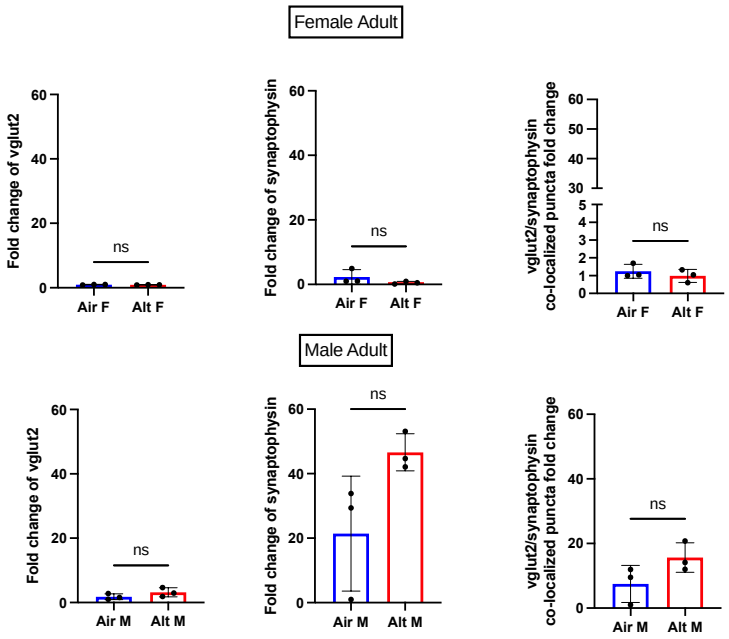

Figure 7: No difference in Pre-Bot zinger regions of mice.

The images (A-L) are stained with Vglut-2 and synaptophysin at PrebotC region of medulla at 63x. (A-C, G-I) is air chamber exposed mice females and males (N= 3 biological sample, n= 1 technical replicates), (D-F, J-L) is A.*altemata* chamber exposure female and male mice (N= 3 biological sample, n= 1 technical replicates). Puncta for colocalization, vglut-2 and synaptophysin were calculated for these images. For females, the colocalization value is p = 0.4543, vglut2 is p = 0.5018, synaptophysin is p = 0.2484. For males, the colocalization is p= 0.1266, vglut2 is p = 0.2283and synaptophysin is p = 0.0801.

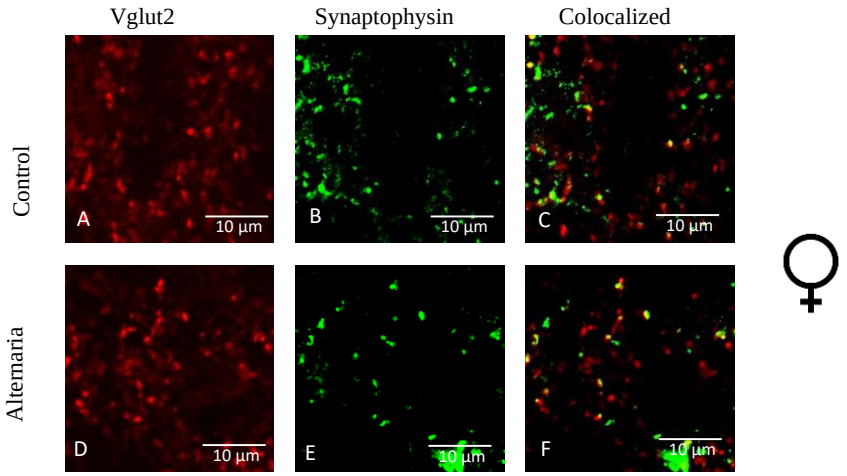
Vglut2
Synaptophysin
Colocalized
Control
Alternaria
A
B
C
D
E
F
10 µm

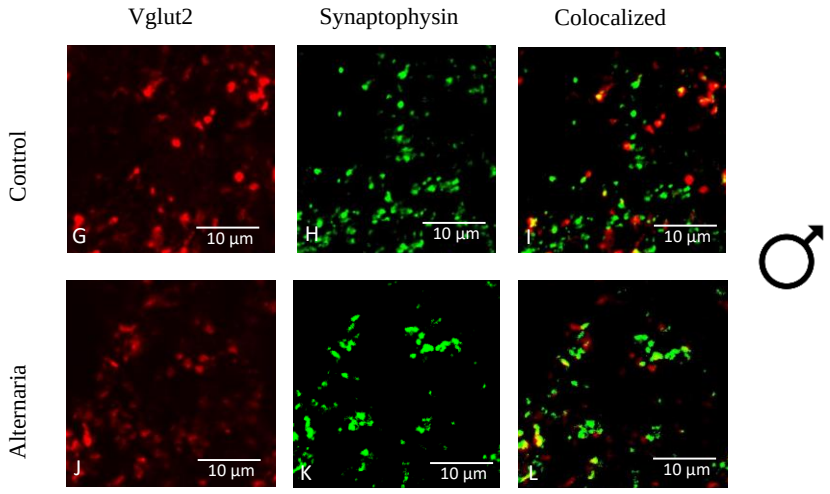
Vglut2
Synaptophysin
Colocalized
Control
Alternaria
G
H
I
J
K
L
10 µm

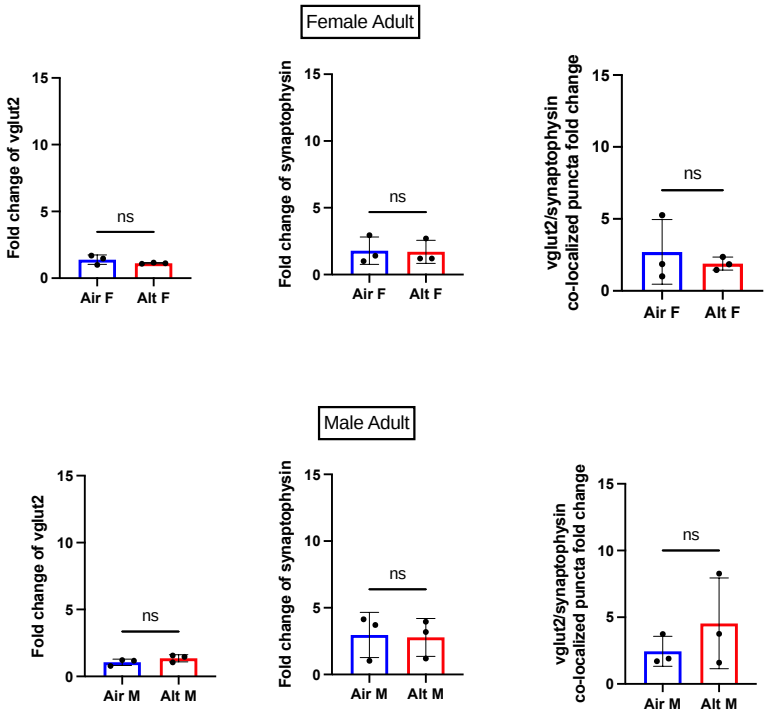

Figure 8: No difference in Bot zinger regions of mice.

The images (A-L) are stained with Vglut-2 and synaptophysin at BotC region of medulla at 63x. (A-C, G-I) is air chamber exposed mice females and males (N= 3 biological sample, n= 1 technical replicates), (D-F, J-L) is A.*alternata* chamber exposure female and male mice (N= 3 biological sample, n= 1 technical replicates). Puncta for colocalization, vglut-2 and synaptophysin were calculated for these images. For females, the colocalization value is p = 0.5722, vglut2 is p = 0.2630, synaptophysin is p = 0.9172. For males, the colocalization is p= 0.3690, vglut2 is p = 0.2249 and synaptophysin is p = 0.8921.

A.*alternata* decreases glutamate transporter EAAT2 expression in females but not in males (Medulla).

EAAT2 is a major glutamate transporter in astrocytes for glutamate uptake. We were able to isolate the medulla region of A. *alternata* exposed and air mice. Using the western blot analysis, the EAAT2 quantification against the total protein stain of the region was analyzed compared to Air mice for both the sexes. In Figure 9A, A.*alternata* exposed females show a decrease in EAAT2 expression compared to Air mice. Males however showed no change in EAAT2 expression when compared to its control subjects (Figure 9B). This analysis suggests that A. *alternata* exposed females are downregulating the major excitatory glutamate receptors of the astrocytes along with the co-localized puncta of vglut2/synaptophysin in Figure (6C, F).

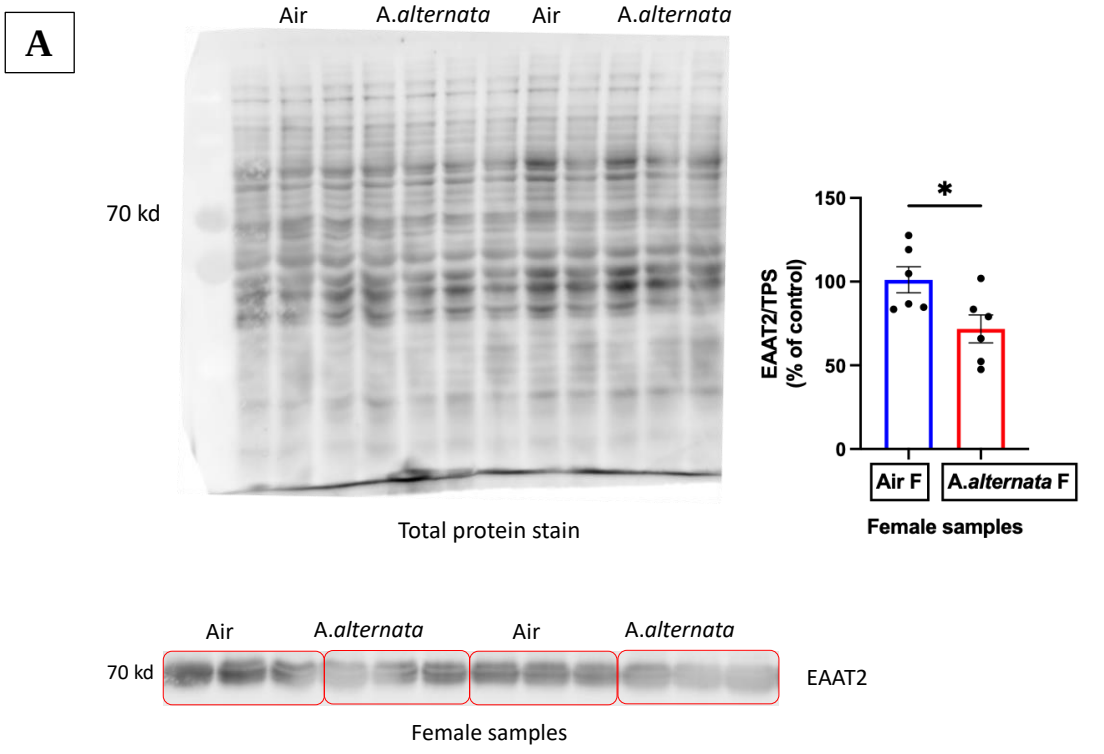
A
Air
A.alternata
Air
A.alternata
70 kd
Total protein stain
EAAT2/TPS (% of control)
150
100
50
0
*
Air F
A.alternata F
Female samples
Air
A.alternata
Air
A.alternata
70 kd
EAAT2
Female samples

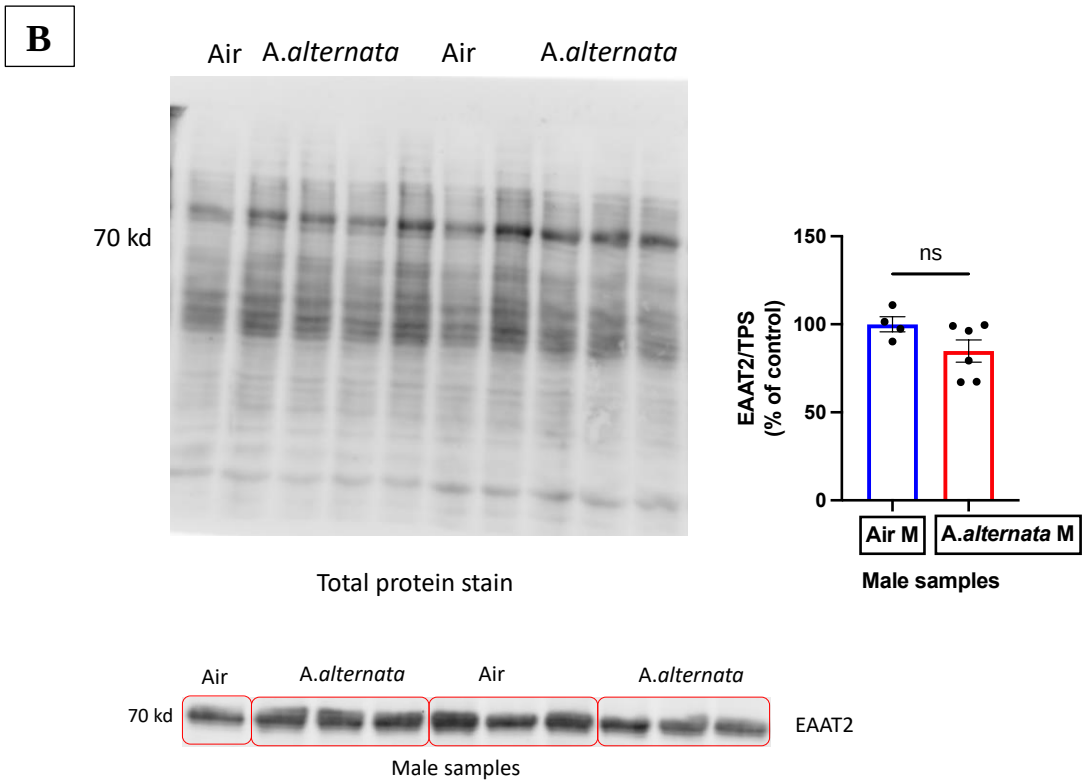
B
Air
A.alternata
Air
A.alternata
70 kd
Total protein stain
EAAT2/TPS (% of control)
150
100
50
0
ns
Air M
A.alternata M
Male samples
Air
A.alternata
Air
A.alternata
70 kd
EAAT2
Male samples

Figure 9: EAAT2 down regulated for A.*alternata* females but not males.

Western blot of two sexes representing the medulla region of the brainstem 8A and 8B. Air females, n= 6 and A.*alternata* females, n = 6. Air males n= 4, and A.*alternata* n= 6. 8A shows the total protein stain of the air and exposed females for normalization and the EAAT2 western blot band detection at 70kd. EAAT2 expression of the A.*alternata* females have decreased by -29.34 ± 11.44 with A.*alternata* females compared to Air females (A). 8B shows total protein stain for air and exposed males for normalization and EAAT2 band detection at 70kd. No significant difference between the Air males and A.*alternata* males (-15.19 ± 8.615).

High-plex protein profiling in the NTS region of the A.*alternata* females and males

Since there are changes in the co-localized vglut2/synaptophysin puncta in females of NTS region, our next approach was to analyze how the neurons and glia cells regulated intracellular cell signaling based on the extracellular environment. The multi-analytic protein experiment shows differential regulation between males and females from the exposure. The exposed females have shown upregulation of phosphorylated GSK3A/B, pan-RAS and downregulation of phosphorylated S6 in Figure 10B. The exposed males are only showing an upregulation of phosphorylated JNK and AMPK-alpha proteins in Figure 10C. A.*alternata* exposed females are the only sex downregulating phosphorylated S6 following the PI3K-Akt pathway signaling. In conclusion both males and females display regulation of molecules in the PI3K-AKT and MAPK signaling pathway, although the molecules significantly regulated differ, with p-S6 being the sole molecule downregulated in exposed females only.

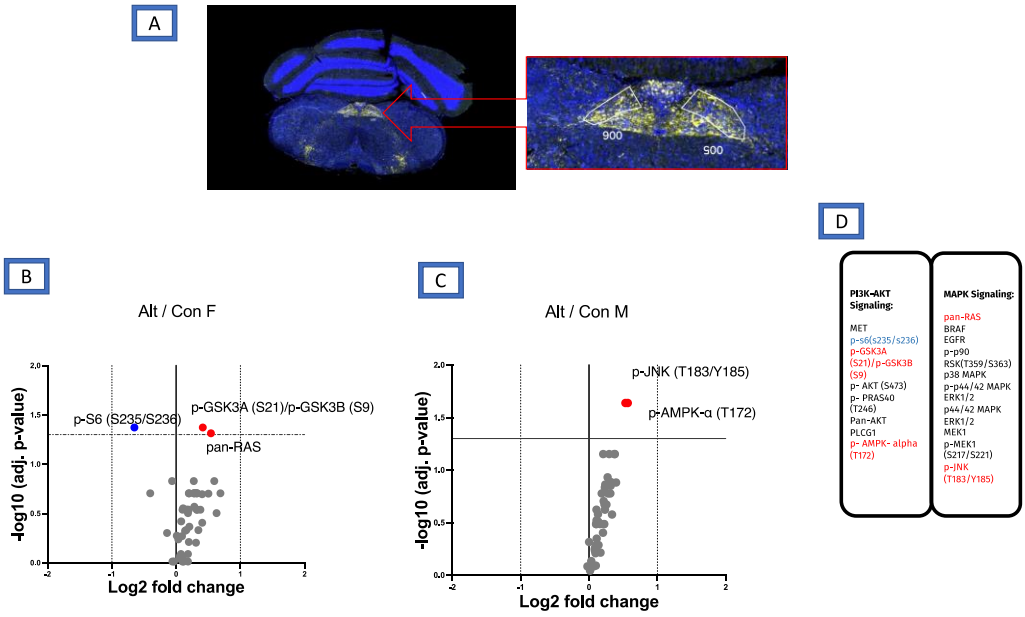

Figure 10: Differential protein regulation of A.*alternata* exposure in NTS region.

The images (A) are stained with panels of personalized tagged antibodies listed in (D) at NTS region of medulla at 63x. Volcano plots of (B) is air chamber exposed female mice and A.*alternata* female chamber exposure mice (N= 6 biological sample), (C) is air chamber exposed male mice and the A.*alternata* male chamber exposed mice (N= 6 biological sample).

Synaptic regulation in Nuclei of the solitary tract (NTS) by LPS 1μg/m^3 (Low Dose)

The LPS aerosolized exposure is a comparison group to see whether the NTS regulation seen in the A.*alternata* exposed group is specific to allergic inflammation or does it also regulate similar changes to innate inflammation by LPS. We first exposed our mice to a lower dose of 1ug/m^3 aerosolized LPS particulates. I cryosectioned the NTS region of adult female and male mice after the 7-day LPS aerosolized chamber exposure, then proceeded to stain the samples with vglut2 and synaptophysin antibodies. Based on the puncta quantification, we saw there were no change in the puncta numbers of vglut2, synaptophysin and co-localization of vglut2/synaptophysin for LPS exposed females and males in Figure 11. This result suggests that the lower dose of LPS might not have a profound effect for synaptic regulation of excitatory presynaptic proteins for both the sexes.

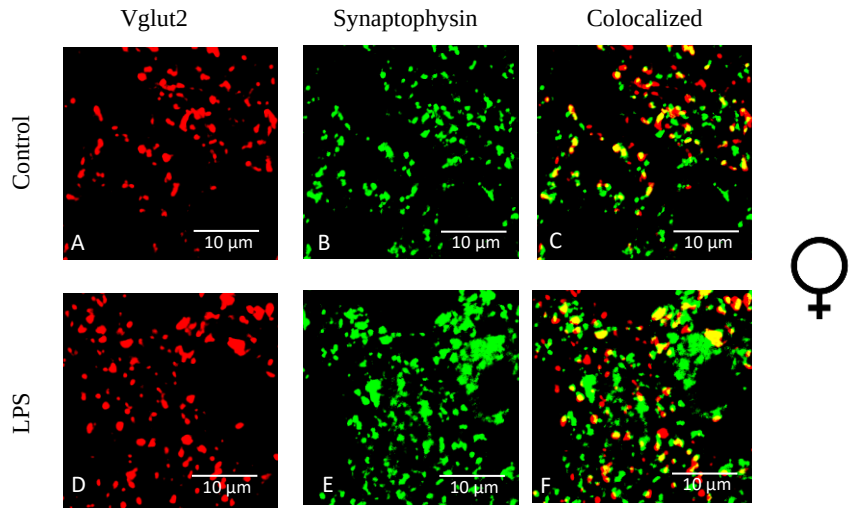
Vglut2
Synaptophysin
Colocalized
Control
LPS
A
B
C
D
E
F
10 µm
♀

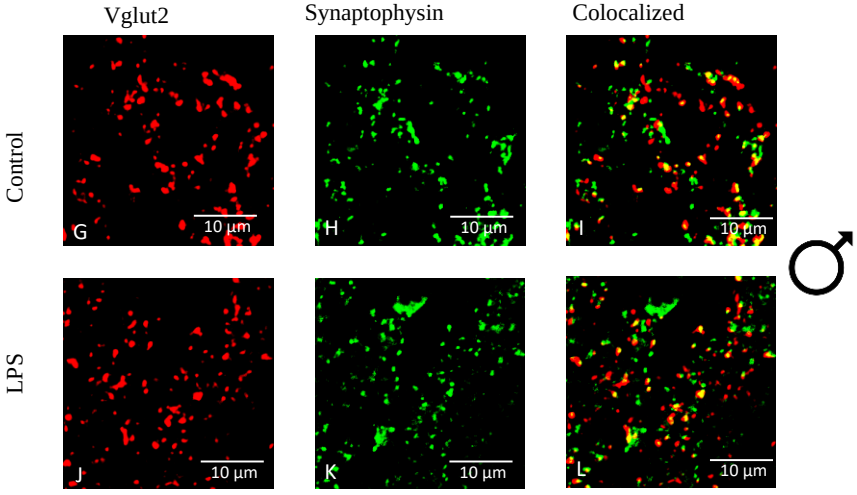
Vglut2
Synaptophysin
Colocalized
Control
LPS
G
H
I
J
K
L
10 µm
♂

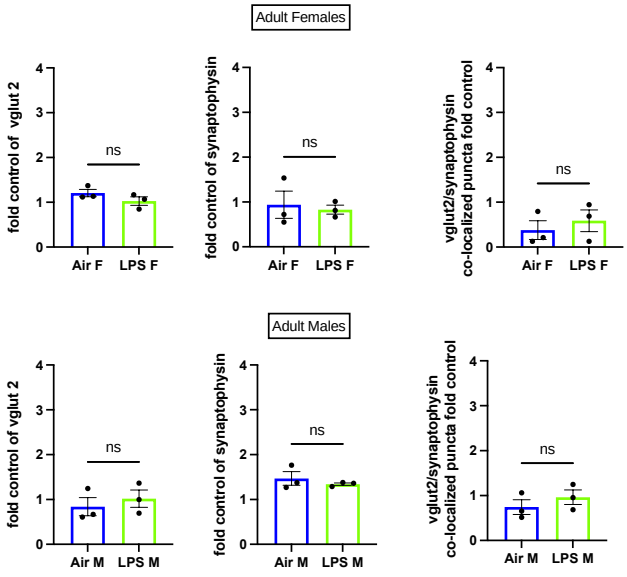

Figure 11: Sex difference in NTS regions of mice of LPS 1 μg/m^3.

The images (A-L) are stained with Vglut-2 and synaptophysin at NTS region of medulla at 63x. (A-C, G-I) is air chamber exposed mice females and males (N= 3 biological sample, n= 3 technical replicates), (D-F, J-L) is LPS chamber exposure female and male mice (N= 3 biological sample, n= 3 technical replicates). Puncta for colocalization, vglut-2 and synaptophysin were calculated for these images. For females, the colocalization value is p = 0.2746, vglut2 is p = 0.1128, synaptophysin is p = 0.7530. For males, the colocalization is p= 0.1982, vglut2 is p = 0.2779 and synaptophysin is p = 0.2285.

High-plex protein profiling in the NTS of the LPS samples at 1μg/m^3 (Low dose)

The next goal was to analyze the NTS region of LPS exposure model to compare A.*alternata* data and see if they both varied in signaling pathway. The exposure at 1ug/m^3 showed to have no significant protein phosphorylation in female exposed mice whereas males showed some proteins expressed under this exposure at seven days' time. Males induced upregulation of proteins related to glial reactivity $CD11b^+$ protein, S100B and Mertk as shown in Figure 12B. In contrast to A.*alternata* exposure, no proteins from the pathways significantly expressed in LPS exposed female mice. Male mice displayed significant induction of glial proteins which was not observed in A.*alternata* exposed male mice. As a result, due to the innate inflammatory exposure to lung, LPS exposed male mice up-regulate proteins markers of the glial cells which is not shown by male mice under allergic inflammation (Figure 10C).

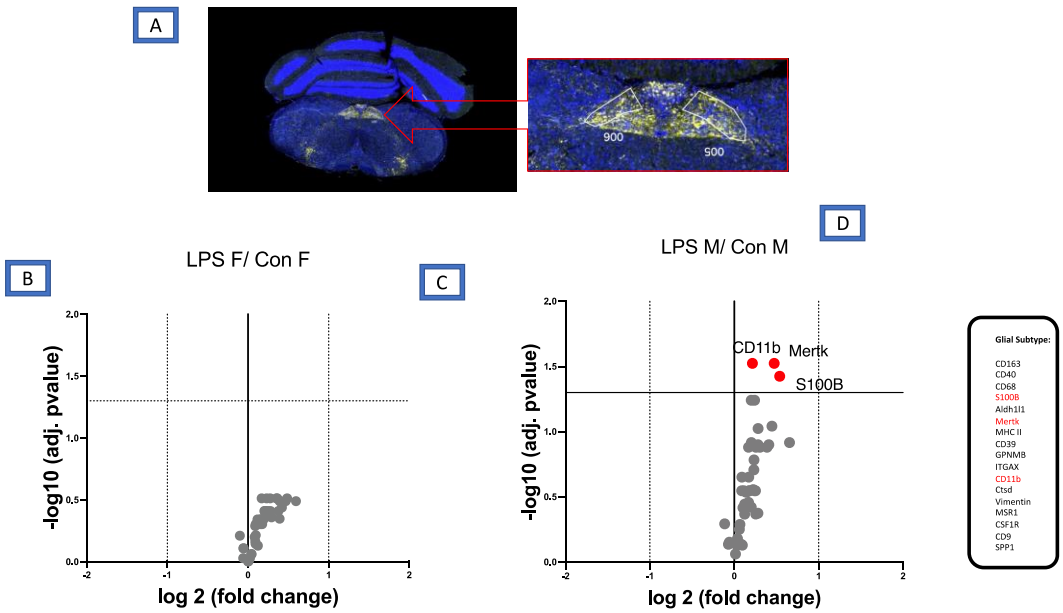

Figure 12: Differential protein regulation in NTS region of low dose LPS.

The images (A) are stained with panels of personalized tagged antibodies listed in (D) at NTS region of medulla at 63x. Volcano plots of (B) is air chamber exposed female mice and LPS female chamber exposure mice (N= 3 biological sample), (C) is air chamber exposed male mice and the LPS male chamber exposed mice (N=3 biological sample).

Synaptic regulation in Nuclei of the solitary tract (NTS) by Lipopolysaccharide at 15 μg/m^3 (High dose)

In figure 11, the lower dose of LPS did not have a stronger response to elicit a synaptic regulation in NTS of both sexes. I decided to expose the mice to a higher dose of aerosolized LPS (15 μg/m^3). Figure 13 shows the NTS region stained with the targeted antibodies and once quantified LPS exposed female mice has shown a significant change in co-localized vglut2/synaptophysin puncta numbers by two-folds compared to the control mice (Figure 13C and 13F). The LPS exposed male mice, however, does not have a significant change in either vglut2, synaptophysin or co-localized puncta numbers compared to its control subjects (Figure 13I and 13L). This result concludes by informing us the changes in synaptic regulation is dose dependent and only females respond to this exposure by changing the synaptic pre-terminal proteins at a higher dose of LPS and shows an opposite effect compared to A. *alternata* exposed female mice (Figure 6C and 6F).

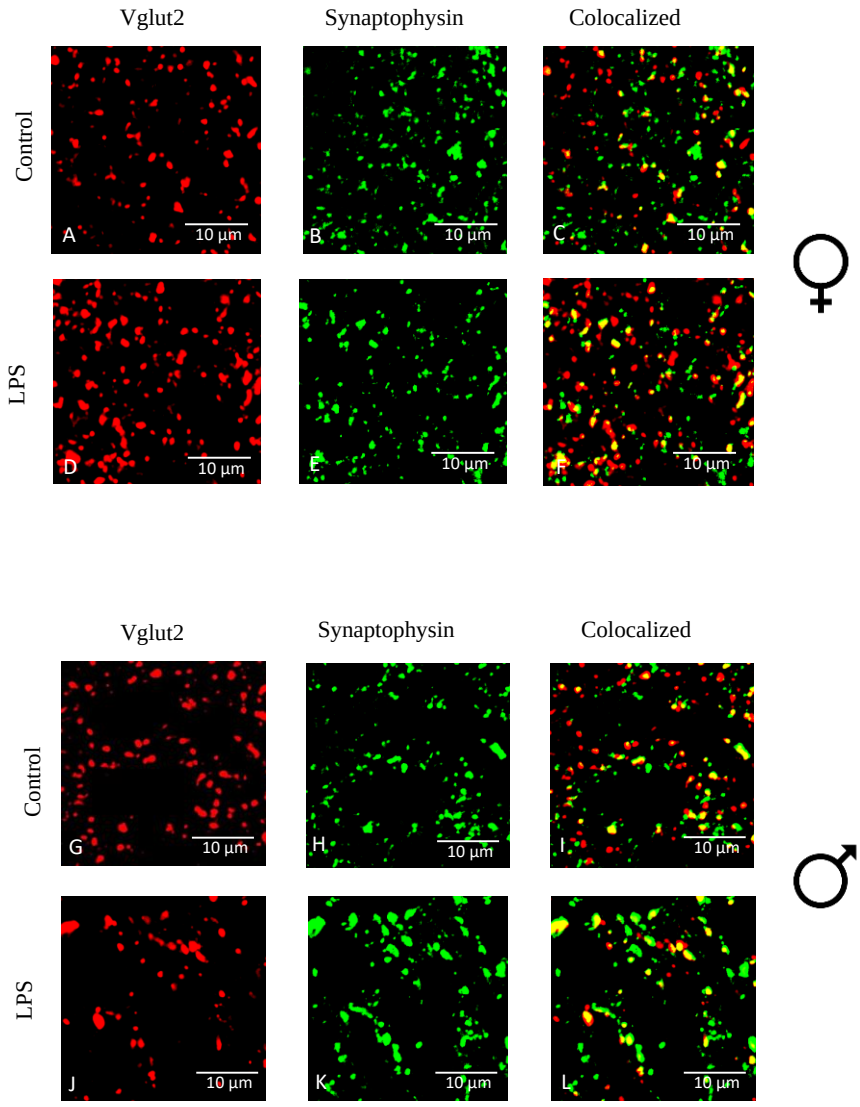
Vglut2
Synaptophysin
Colocalized
Control
LPS
A
B
C
D
E
F
10 µm
♀
Vglut2
Synaptophysin
Colocalized
Control
LPS
G
H
I
J
K
L
10 µm
♂

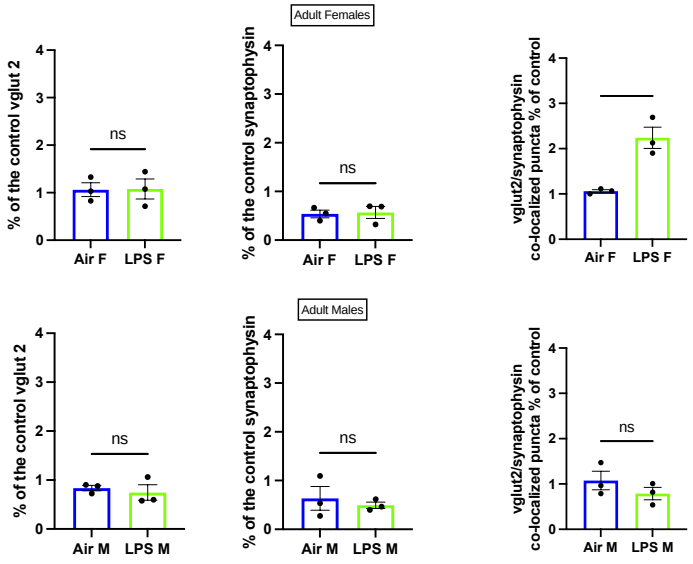

Figure 13: Sex difference in NTS regions of mice of LPS 15 μg/m^3.

The images (A-L) are stained with Vglut-2 and synaptophysin at NTS region of medulla at 63x. (A-C, G-I) is air chamber exposed mice females and males (N= 3 biological sample, n= 3 technical replicates), (D-F, J-L) is LPS chamber exposure female and male mice (N= 3 biological sample, n= 3 technical replicates). Puncta for colocalization, vglut-2 and synaptophysin were calculated for these images. For females, the colocalization value is p = 0.0077*, vglut2 is p = 0.9552, synaptophysin is p = 0.8455. For males, the colocalization is p= 0.3090, vglut2 is p = 0.7465 and synaptophysin is p = 0.6042.

High-plex protein profiling in the NTS of the LPS samples at 15μg/m^3 (High dose)

The two-fold increase of co-localized female puncta in figure 13 then encourages us to ask how the signaling cascades between the neurons and glial cells are regulated under the high dose LPS exposure. The NTS region was quantified using the high-plex protein analysis and there was different protein regulation within the exposed males and female mice. LPS exposed male mice showed no significant protein regulation based on the five panels we chose (Figure 14C). The exposed female mice showed downregulation of proteins such as MEK1 and ITGAX (Figure 14B). MEK1 is a protein associated with MAPK signaling pathway and ITGAX is a protein encoded for microglial $CD11c^+$ subsets. This protein regulation is important to understand since we are also seeing a two-fold increase in co-localized puncta fold change of both vglut2 and synaptophysin in A.*alternata* exposed females (Figure 13C).

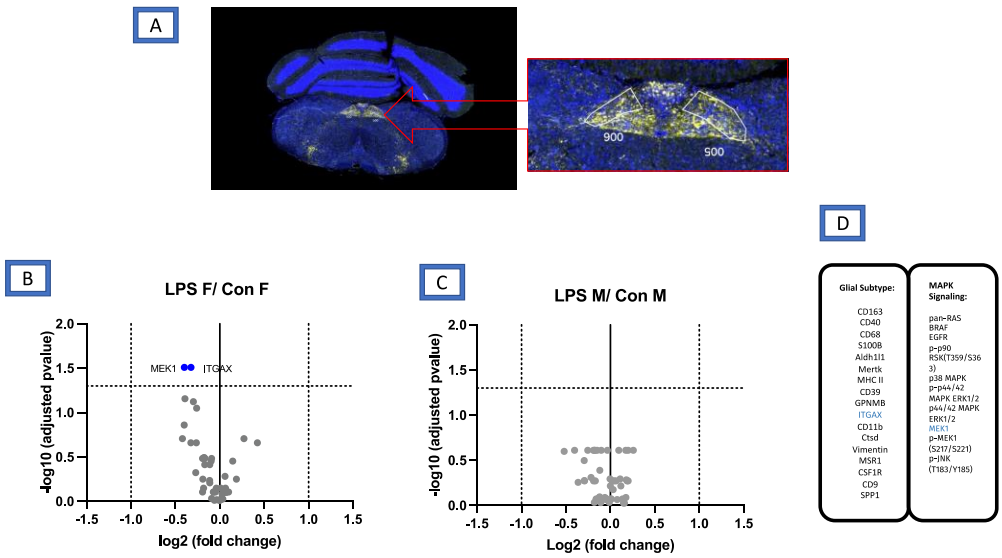

Figure 14: Differential protein regulation in NTS region of high dose LPS.

The images (A) are stained with panels of personalized tagged antibodies listed in (D) at NTS region of medulla at 63x. Volcano plots of (B) is air chamber exposed female mice and LPS female chamber exposure mice (N= 3 biological sample), (C) is air chamber exposed male mice and the LPS male chamber exposed mice (N=3 biological sample).

Discussion:

The observed results are showing insightful information on how each sex is regulating the NTS synaptic terminals based on the exposures used. The exposures are the bigger influences in the differences we are seeing here while the sex difference is still being considered.

A.*alternata* exposed mice:

Administration of fungal aerosolized particulate exposure to our C57BL/6J mice, we see no synaptic changes at presynaptic protein marker expression to glutamate release for exposed males. A decrease in colocalized vglut2/synaptophysin puncta and EAAT2 expression is seen in A.*alternata* exposed females. This could suggest A.*alternata* exposed females are responding more to the adaptive immune response from lung by regulating less glutamate release whereas exposed males do not have to regulate any presynaptic proteins for glutamatergic signaling release from the lung inflammation. Similarly, the cell signaling cascade also shows a sex-specific effect that might be eliciting the females to respond more to this exposure compared to males. Females are upregulating proteins that are linked to PI3K-AKT and MAPK signaling cascades where phosphorylation of AKT also activates the isoforms of GSK3 alpha/beta to regulate apoptosis or any neuronal degeneration. GSK3 alpha/beta is negatively phosphorylated by protein kinase B (AKT) on their tyrosine residues Ser 21 and Ser 9 (Matsuda et al., 2019). Studies have shown the negative phosphorylated regulation of GSK3 in axonal remodeling of neuronal cultures in cerebellar regions (Lucas & Salinas, 1997). GSK3 is responsible for many neuronal functions and phosphorylation of this proteins is to maintain synapse homeostasis and synaptogenesis. For example, the activation of NMDAR receptors in hippocampal neurons will inhibit GSK3 by Ser 9 phosphorylation (Peineau et al., 2007). Therefore, they have implications in release of glutamate release. The up regulation of these proteins might be an indication of controlling the decrease in co-localized puncta through regulation of glutamate receptors and

presynaptic proteins of A.*alternata* exposed females. Knight et al., showed that ribosomal S6 undergoes post-translation modifications when neurons receives different stimulus (Knight et al., 2012). Our protein analysis shows downregulation of phosphorylated ribosomal S6 of A.*alternata* exposed females which might indicate less glutamatergic signaling excitation of neurons in the NTS and decrease in their co-localized puncta quantification. Even though we did not detect any significant changes in synaptic puncta for males, they show a differential regulation of proteins in cell signaling cascades. A.*alternata* exposed males also showed upregulation of proteins from both the cascades, but different expression of proteins compared to A.*alternata* exposed females. A.*alternata* exposed males shows an up-regulation of phosphorylated JNK T172, a downstream signaling of MAPK cascade. JNK along with JIPI scaffold protein is known to regulate NMDAR receptors in presence of glutamate excitotoxicity, and this could be in conjunction with what I am seeing at puncta quantification and why there is no significant change in males (Morel et al., 2018). It is important to state the presynaptic protein puncta are not significantly regulated in the BotC and preBotC regions of exposed males and females. This could explain that the regulation of the adaptive inflammation is controlled at the NTS region and does not to be regulated further to the complexes for the exposed females. Concluding with A.*alternata* data, we can see that exposed females are regulating the synaptic plasticity more than exposed males in the presence of an non-infectious allergic inflammation.

Lipopolysaccharide exposed mice:

Using LPS innate inflammatory exposure have not only shown a differential regulation of puncta and cascade signaling compared to A.*alternata* but also sex differences among them.

At a lower dose LPS, there were no changes in the presynaptic terminal glutamatergic protein regulation in neither male nor female exposed mice. In addition to this, the GeoMX

analysis showed that there was no significant protein phosphorylated in low dose LPS exposed females. Low dose LPS exposed males showed proteins upregulated from glial-cell subtyping panels such as MertK, S100B and CD11b. S100b is a peptide that acts as CA^{2+} sensors for peptides that is released and protects hippocampal neurons from glutamate excitotoxicity, however correlation between glutamate and S100B is unclear even though astrocytes have bigger responsibility of glutamate clearance. Tramontina F et al., have showed a correlation between high glutamate release and a decrease level of s100B and suggest that the toxicity of glutamate might severe the cylic AMP levels from metabotropic receptors activation causing a lower release of s100b (Tramontina et al., 2006). In our data, the presynaptic VGLUT2 and synaptophysin is not significantly regulated in the NTS region of both the exposed females and males hence dictate no excitotoxity of glutamate release. $Cd11b^{+}$ is a marker of microglia and Mertk is a phagocytic receptor expressed by microglia and is responsible in phagocytosis of synaptic terminals activated by "eat-me" signals from neurons. (Park et al., 2021) have shown the involvement of MerTK receptors in inhibitory post synapse elimination. They showed the colocalization of gephyrin positive markers, a post inhibitory post-synaptic element, inside microglial CD68 positive lysosome markers in a knockout model of *Cdc50a* mice. They further analyzed excitatory and inhibitory synapses for *Cdc50a* mice model in the cortex, hippocampus and inferior colliculus and have shown a decrease in gephyrin/VGAT inhibitory protein colocalization but no change in excitatory PSD9/VGLUT1 protein colocalization further solidifying the microglial MERTK involvement in inhibitory synapses of the *Cdc50a* mice model (Park et al., 2021). Our data shows no change in the excitatory presynaptic colocalization of Vglut2/synaptophysin puncta of exposed males might indicate regulation of other neurotransmitter under this exposure, however, this requires experiments related to inhibitory synapses. Even though these studies are extreme in the sense of triggering neuronal toxicity, our mice showed no significant regulation in synaptic

plasticity implicating that the glial protein upregulation under low dose LPS exposed males only, are in homeostasis surveilling the environment. In conclusion, they might be doing it by clearance of glutamate by microglia and an increase in S100B concentration due to the phagocytotic activity of glutamate by microglia and less glutamate presence in the synaptic cleft.

At a higher dose of LPS exposure, exposed females showed a two-fold increase in colocalized vglut2/synaptophysin puncta whereas no significant regulation in exposed male mice. This regulation can be explained from the protein analysis we obtained at the NTS region. High dose LPS female shows a downregulated expression of unphosphorylated MEK1 protein. When the MEK1 is phosphorylated, it activates the MAPK signaling, it is implicated to phosphorylate major proteins downstream such as extracellular signal-regulated kinase 1/2 (ERK1/2) to regulate NMDA receptors from excitatory glutamate neurotransmitter and promote neuronal survival (Cook et al., 2011). The co-localized vglut2 and synaptophysin puncta increase might implicate an increase in glutamate release onto the synaptic cleft and this further reinforce with our protein analysis data. Since we are seeing mitogen activated protein kinase 1 (MEK1) protein being downregulated, it is plausible that the cause of the two-fold increase in puncta is due to unphosphorylated MEK1 protein inhibiting the downstream signaling cascade MAPK from trigger of glutamate excitotoxicity. MEK1 is activated by Raf kinases when phosphorylated at the S217 and S221 for it's role in neuronal damage (Krepinsky et al., 2002). However, in our case MEK1 is not being phosphorylated at it's serine site. Studies have shown that phosphorylation of MEK1 and further activation of MAPK signal is due to depolarization of the neuron terminals and influx of calcium signaling, it is plausible in our case the high dose LPS exposed females are downregulating this protein to decrease the influx of calcium which then would decrease the release of glutamate neurotransmitters to protect its neuronal environment, however we need to do more experiments to further demonstrate this result (Rosen et al., 1994). Concurrently, we are

also seeing a downregulation of ITGAX a gene promoter for $CD11c^{+}$ dendritic cells (Prodinger et al., 2011). Even though dendritic cells are present in the choroid plexus which respond to antigen presenting molecules in the cerebrospinal fluid, the higher dose LPS exposure is an activation of an innate inflammation in the lung solely by neutrophil recruitment as shown by Biddle et al. (Biddle et al., 2023). It is important to understand that the NTS region is in the proximity of area postrema region of medulla oblongata and caudal to fourth ventricle outside of blood brain barrier (Scott, 2002). The downregulation of the ITGAX in high LPS dose exposed females may influence an increase in co-localized vglut2/synaptophysin puncta. This is a suggestion that the dendritic cells might be recruited around the NTS region are being downregulated. On the other hand, high dose exposed males shows neither significant puncta nor protein regulation.

The data obtained shows some exciting evidence on understanding sex differences based on different exposure of particulates. Higher dose LPS exposed females increases co-localized puncta whereas A. a*lternata* female mice decreases co-localized puncta. Males showed no significant regulation in the vglut2, synaptophysin and vglut2/synaptophysin co-localized puncta quantification from both types of exposures of the A. *alternata* and the two doses of LPS aerosolized exposure. The data shows that females are responding more to the exposures meanwhile altering the presynaptic proteins differently based on the exposures. Even though the males did not show any regulation at synaptic terminals, their signaling cascades are differently regulated than that of their female mice cohorts. The data obtained further solidifies about the difference in the innate and adaptive inflammation in female and male mice as shown by puncta quantification and high-throughput protein analysis.

Reference:

Abdel Rasheed, N. O., & Ibrahim, W. W. (2022). Telmisartan neuroprotective effects in 3-nitropropionic acid Huntington's disease model in rats: Cross talk between PPAR-γ and PI3K/Akt/GSK-3β pathway. *Life Sciences*, *297*, 120480.

Amato, S., & Man, H.-Y. (2011). Bioenergy sensing in the brain: the role of AMP-activated protein kinase in neuronal metabolism, development and neurological diseases. *Cell Cycle* , *10*(20), 3452–3460.

Balan, K. V., Kc, P., Hoxha, Z., Mayer, C. A., Wilson, C. G., & Martin, R. J. (2011). Vagal afferents modulate cytokine-mediated respiratory control at the neonatal medulla oblongata. *Respiratory Physiology & Neurobiology*, *178*(3), 458–464.

Bertani, B., & Ruiz, N. (2018). Function and Biogenesis of Lipopolysaccharides. *EcoSal Plus*, *8*(1). https://doi.org/10.1128/ecosalplus.ESP-0001-2018

Biddle, T. A., Li, Q., Maltz, M. R., Tandel, P. N., Chakraborty, R., Yisrael, K., Drover, R., Cocker, D. R., 3rd, & Lo, D. D. (2021). Salton Sea aerosol exposure in mice induces a pulmonary response distinct from allergic inflammation. *The Science of the Total Environment*, *792*, 148450.

Biddle, T. A., Yisrael, K., Drover, R., Li, Q., & Maltz, M. R. (2023). Aerosolized aqueous dust extracts collected near a drying lake trigger acute neutrophilic pulmonary inflammation reminiscent of microbial innate immune …. *The Science of the Total Environment*. https://www.sciencedirect.com/science/article/pii/S0048969722069820

Cadwell, K. (2016). Crosstalk between autophagy and inflammatory signalling pathways: balancing defence and homeostasis. *Nature Reviews. Immunology*, *16*(11), 661–675.

Carson, M. J., Doose, J. M., Melchior, B., Schmid, C. D., & Ploix, C. C. (2006). CNS immune privilege: hiding in plain sight. *Immunological Reviews*, *213*, 48–65.

Colton, C. A. (2013). Immune heterogeneity in neuroinflammation: dendritic cells in the brain. *Journal of Neuroimmune Pharmacology: The Official Journal of the Society on NeuroImmune Pharmacology*, *8*(1), 145–162.

Cook, D. R., Gleichman, A. J., Cross, S. A., Doshi, S., Ho, W., Jordan-Sciutto, K. L., Lynch, D. R., & Kolson, D. L. (2011). NMDA receptor modulation by the neuropeptide apelin: implications for excitotoxic injury. *Journal of Neurochemistry*, *118*(6), 1113–1123.

Ersahin, T., Tuncbag, N., & Cetin-Atalay, R. (2015). The PI3K/AKT/mTOR interactive pathway. *Molecular BioSystems*, *11*(7), 1946–1954.

Gakis, G., Mueller, M. H., Hahn, J., Glatzle, J., Grundy, D., & Kreis, M. E. (2009). Neuronal activation in the nucleus of the solitary tract following jejunal lipopolysaccharide in the rat. *Autonomic Neuroscience: Basic & Clinical*, *148*(1–2), 63–68.

Hiroki, C. H., Sarden, N., Hassanabad, M. F., & Yipp, B. G. (2021). Innate Receptors Expression by Lung Nociceptors: Impact on COVID-19 and Aging. *Frontiers in Immunology*, *12*, 785355.

Holgate, S. T. (2008). Pathogenesis of asthma. *Clinical and Experimental Allergy: Journal of the British Society for Allergy and Clinical Immunology*, *38*(6), 872–897.

Hwang, J.-Y., Yan, J., & Zukin, R. S. (2019). Autophagy and synaptic plasticity: epigenetic regulation. *Current Opinion in Neurobiology*, *59*, 207–212.

Jaillon, S., Berthenet, K., & Garlanda, C. (2019). Sexual Dimorphism in Innate Immunity. *Clinical Reviews in Allergy & Immunology*, *56*(3), 308–321.

Kim, H.-K., Lund, S., Baum, R., Rosenthal, P., Khorram, N., & Doherty, T. A. (2014). Innate type 2 response to Alternaria extract enhances ryegrass-induced lung inflammation. *International Archives of Allergy and Immunology*, *163*(2), 92–105.

Klein, S. L., & Flanagan, K. L. (2016). Sex differences in immune responses. *Nature Reviews. Immunology*, *16*(10), 626–638.

Kline, D. D. (2008). Plasticity in glutamatergic NTS neurotransmission. *Respiratory Physiology & Neurobiology*, *164*(1–2), 105–111.

Knight, Z. A., Tan, K., Birsoy, K., Schmidt, S., Garrison, J. L., Wysocki, R. W., Emiliano, A., Ekstrand, M. I., & Friedman, J. M. (2012). Molecular profiling of activated neurons by phosphorylated ribosome capture. *Cell*, *151*(5), 1126–1137.

Knutsen, A. P., Bush, R. K., Demain, J. G., Denning, D. W., Dixit, A., Fairs, A., Greenberger, P. A., Kariuki, B., Kita, H., Kurup, V. P., Moss, R. B., Niven, R. M., Pashley, C. H., Slavin, R. G., Vijay, H. M., & Wardlaw, A. J. (2012). Fungi and allergic lower respiratory tract diseases. *The Journal of Allergy and Clinical Immunology*, *129*(2), 280–291; quiz 292–293.

Krepinsky, J., Wu, D., Ingram, A., Scholey, J., & Tang, D. (2002). Developments in mitogen-induced extracellular kinase 1 inhibitors and their use in the treatment of disease. *Expert Opinion on Therapeutic Patents*, *12*(12), 1795–1811.

Limanaqi, F., Busceti, C. L., Celli, R., Biagioni, F., & Fornai, F. (2021). Autophagy as a gateway for the effects of methamphetamine: From neurotransmitter release and synaptic plasticity to psychiatric and neurodegenerative disorders. *Progress in Neurobiology*, *204*, 102112.

Liu, E., Xie, A.-J., Zhou, Q., Li, M., Zhang, S., Li, S., Wang, W., Wang, X., Wang, Q., & Wang, J.-Z. (2017). GSK-3β deletion in dentate gyrus excitatory neuron impairs synaptic plasticity and memory. *Scientific Reports*, *7*(1), 5781.

Long, H.-Z., Cheng, Y., Zhou, Z.-W., Luo, H.-Y., Wen, D.-D., & Gao, L.-C. (2021). PI3K/AKT Signal Pathway: A Target of Natural Products in the Prevention and Treatment of Alzheimer's Disease and Parkinson's Disease. *Frontiers in Pharmacology*, *12*, 648636.

Lucas, F. R., & Salinas, P. C. (1997). WNT-7a induces axonal remodeling and increases synapsin I levels in cerebellar neurons. *Developmental Biology*, *192*(1), 31–44.

Mahmoud, S., Gharagozloo, M., Simard, C., & Gris, D. (2019). Astrocytes Maintain Glutamate Homeostasis in the CNS by Controlling the Balance between Glutamate Uptake and Release. *Cells* , *8*(2). https://doi.org/10.3390/cells8020184

Martin, S. A., Pence, B. D., Greene, R. M., Johnson, S. J., Dantzer, R., Kelley, K. W., & Woods, J. A. (2013). Effects of voluntary wheel running on LPS-induced sickness behavior in aged mice. *Brain, Behavior, and Immunity*, *29*, 113–123.

Mascarucci, P., Perego, C., Terrazzino, S., & De Simoni, M. G. (1998). Glutamate release in the nucleus tractus solitarius induced by peripheral lipopolysaccharide and interleukin-1 beta. *Neuroscience*, *86*(4), 1285–1290.

Matsuda, S., Ikeda, Y., Murakami, M., Nakagawa, Y., Tsuji, A., & Kitagishi, Y. (2019). Roles of PI3K/AKT/GSK3 Pathway Involved in Psychiatric Illnesses. *Diseases (Basel, Switzerland)*, *7*(1). https://doi.org/10.3390/diseases7010022

Morel, C., Sherrin, T., Kennedy, N. J., Forest, K. H., Avcioglu Barutcu, S., Robles, M., Carpenter-Hyland, E., Alfulaij, N., Standen, C. L., Nichols, R. A., Benveniste, M., Davis, R. J., & Todorovic, C. (2018). JIP1-Mediated JNK Activation Negatively Regulates Synaptic Plasticity and Spatial Memory. *The Journal of Neuroscience: The Official Journal of the Society for Neuroscience*, *38*(15), 3708–3728.

Neher, J. J., Emmrich, J. V., Fricker, M., Mander, P. K., Théry, C., & Brown, G. C. (2013). Phagocytosis executes delayed neuronal death after focal brain ischemia. *Proceedings of the National Academy of Sciences of the United States of America*, *110*(43), E4098-107.

Nguyen, A. Q., Sutley, S., Koeppen, J., Mina, K., Woodruff, S., Hanna, S., Vengala, A., Hickmott, P. W., Obenaus, A., & Ethell, I. M. (2020). Astrocytic Ephrin-B1 Controls Excitatory-Inhibitory Balance in Developing Hippocampus. *The Journal of Neuroscience: The Official Journal of the Society for Neuroscience*, *40*(36), 6854–6871.

Paolicelli, R. C., Sierra, A., Stevens, B., Tremblay, M.-E., Aguzzi, A., Ajami, B., Amit, I., Audinat, E., Bechmann, I., Bennett, M., Bennett, F., Bessis, A., Biber, K., Bilbo, S., Blurton-Jones, M., Boddeke, E., Brites, D., Brône, B., Brown, G. C., … Wyss-Coray, T. (2022). Microglia states and nomenclature: A field at its crossroads. *Neuron*, *110*(21), 3458–3483.

Park, J., Choi, Y., Jung, E., Lee, S.-H., Sohn, J.-W., & Chung, W.-S. (2021). Microglial MERTK eliminates phosphatidylserine-displaying inhibitory post-synapses. *The EMBO Journal*, *40*(15), e107121.

Peineau, S., Taghibiglou, C., Bradley, C., Wong, T. P., Liu, L., Lu, J., Lo, E., Wu, D., Saule, E., Bouschet, T., Matthews, P., Isaac, J. T. R., Bortolotto, Z. A., Wang, Y. T., & Collingridge, G. L. (2007). LTP inhibits LTD in the hippocampus via regulation of GSK3beta. *Neuron*, *53*(5), 703–717.

Peng, X., Madany, A. M., Jang, J. C., Valdez, J. M., Rivas, Z., Burr, A. C., Grinberg, Y. Y., Nordgren, T. M., Nair, M. G., Cocker, D., Carson, M. J., & Lo, D. D. (2018). Continuous Inhalation Exposure to Fungal Allergen Particulates Induces Lung Inflammation While Reducing Innate Immune Molecule Expression in the Brainstem. *ASN Neuro*, *10*, 1759091418782304.

Prodinger, C., Bunse, J., Krüger, M., Schiefenhövel, F., Brandt, C., Laman, J. D., Greter, M., Immig, K., Heppner, F., Becher, B., & Bechmann, I. (2011). CD11c-expressing cells reside in the juxtavascular parenchyma and extend processes into the glia limitans of the mouse nervous system. *Acta Neuropathologica*, *121*(4), 445–458.

Qin, Y., Zhu, Y., Baumgart, J. P., Stornetta, R. L., Seidenman, K., Mack, V., van Aelst, L., & Zhu, J. J. (2005). State-dependent Ras signaling and AMPA receptor trafficking. *Genes & Development*, *19*(17), 2000–2015.

Rosen, L. B., Ginty, D. D., Weber, M. J., & Greenberg, M. E. (1994). Membrane depolarization and calcium influx stimulate MEK and MAP kinase via activation of Ras. *Neuron*, *12*(6), 1207–1221.

Salo, P. M., Arbes, S. J., Jr, Sever, M., Jaramillo, R., Cohn, R. D., London, S. J., & Zeldin, D. C. (2006). Exposure to Alternaria alternata in US homes is associated with asthma symptoms. *The Journal of Allergy and Clinical Immunology*, *118*(4), 892–898.

Scott, D. E. (2002). Ventricular System. In V. S. Ramachandran (Ed.), *Encyclopedia of the Human Brain* (pp. 661–685). Academic Press.

Shen, X., Qiu, Y., Wight, A. E., Kim, H.-J., & Cantor, H. (2022). Definition of a mouse microglial subset that regulates neuronal development and proinflammatory responses in the brain. *Proceedings of the National Academy of Sciences of the United States of America*, *119*(8). https://doi.org/10.1073/pnas.2116241119

Tramontina, F., Leite, M. C., Gonçalves, D., Tramontina, A. C., Souza, D. F., Frizzo, J. K., Nardin, P., Gottfried, C., Wofchuk, S. T., & Gonçalves, C.-A. (2006). High glutamate decreases S100B secretion by a mechanism dependent on the glutamate transporter. *Neurochemical Research*, *31*(6), 815–820.

Wei, J., Liu, W., & Yan, Z. (2010). Regulation of AMPA Receptor Trafficking and Function by Glycogen Synthase Kinase 3 *. *The Journal of Biological Chemistry*, *285*(34), 26369–26376.

White, D. N., & Stowell, M. H. B. (2021). Room for Two: The Synaptophysin/Synaptobrevin Complex. *Frontiers in Synaptic Neuroscience*, *13*, 740318.

Yackle, K. (2023). Transformation of Our Understanding of Breathing Control by Molecular Tools. *Annual Review of Physiology*, *85*, 93–113.

Zhu, C., Xu, F., Wang, X., Shibata, M., Uchiyama, Y., Blomgren, K., & Hagberg, H. (2006). Different apoptotic mechanisms are activated in male and female brains after neonatal hypoxia-ischaemia. *Journal of Neurochemistry*, *96*(4), 1016–1027.

Zhu, L.-Q., Liu, D., Hu, J., Cheng, J., Wang, S.-H., Wang, Q., Wang, F., Chen, J.-G., & Wang, J.-Z. (2010). GSK-3 beta inhibits presynaptic vesicle exocytosis by phosphorylating P/Q-type calcium channel and interrupting SNARE complex formation. The Journal of Neuroscience: The Official Journal of the Society for Neuroscience, 30(10), 3624–3633.